THE UNIV. OF MICH.
DEC 21 1961
PHYSICS LIBRARY

REGISTERED No. BG. 315

PROCEEDINGS

OF THE

INDIAN ACADEMY OF SCIENCES

VOL. LIV] *SECTION A* [No. 4

OCTOBER 1961

Price Rs. 2 or 3 Sh. *Annual Subscription Rs. 18*

IMPORTANT

Notice to the Subscribers of the "Proceedings of the Indian Academy of Sciences"

As from 1st January 1962, the following subscription prices for the *Proceedings of the Indian Academy of Sciences* will come into effect:—

Annual Subscription Rates

	Sections A & B	Section A	Section B
Inland ..	Rs. 72 00 nP.	Rs. 36 00 nP.	Rs. 36 00 nP.
Foreign ..	$ 18 00 cts.	$ 9 00 cts.	$ 9 00 cts.
	or	or	or
..	£ 6-0-0	£ 3-0-0	£ 3-0-0

The *Proceedings of the Indian Academy of Sciences*, a monthly, which commenced its publication in July 1934 in two Sections, A and B, comprising of papers in physical and biological sciences respectively, has since then maintained an unbroken record of punctual issue on the last date of every month. Two volumes in each Section are issued every year and the 54th volume is now running. Each volume contains between pages 350 to 400 of text, 15 to 20 full-page plates and a large number of figures in the text. The *Proceedings* embody the results of the scientific research of the highest quality carried out in India.

The subscription price, which was originally fixed in July 1934, has remained unaltered all these years. The printing costs have progressively increased and are at present nearly three times the original ones. It has therefore become inevitable that the subscription rates are enhanced to enable the *Proceedings* to continue to offer to our subscribers the same volume of material and the same quality of paper, printing and illustrations as at present.

PRINTED AT THE BANGALORE PRESS, BANGALORE CITY, BY T. K. BALAKRISHNAN, SUPERINTENDENT, AND PUBLISHED BY THE INDIAN ACADEMY OF SCIENCES, BANGALORE

SOME EFFECTS OF GEOMAGNETIC ACTIVITY ON THE F2 REGION OF THE IONOSPHERE OVER LEOPOLDVILLE (4·4° S, 15·3° E)

By R. G. Rastogi

(High Altitude Observatory, University of Colorado, Boulder, Colorado)

Received August 16, 1961

(Communicated by Prof. Sydney Chapman, Hon. F.A.Sc.)

The solar diurnal variation of the critical frequency of the F2 layer, foF2, has been shown by Rastogi (1959) to be very different at stations having the same geomagnetic, but different magnetic latitudes. The value of foF2 at Ibadan (geomagnetic latitude = 10° N) reaches two maxima in the morning and in the evening hours during the years of low solar activity, a feature characteristic of the equatorial stations. However, at Leopoldville, the diurnal variation of foF2 shows a single afternoon peak, a feature characteristic of temperate latitude stations (Rastogi, 1960). These features of foF2 at Ibadan and Leopoldville are consistent with the magnetic latitudes of the stations being 2·5° S and 19° S respectively.

In a later communication, Rastogi (1961) showed that the lunar semi-diurnal variation of midday foF2 at Leopoldville has maximum positive deviation at about 11 lunar hours whereas the same at Ibadan is found by Brown (1956) to occur at about 03 lunar hours. It was shown that a similar type of lunar semi-diurnal variation of foF2 is observed at stations having the same magnetic latitudes.

In view of the large differences in the solar and lunar variations of foF2 at Ibadan and Leopoldville, a comparison is made in this paper of the effect of geomagnetic disturbances in the F2 region of the ionosphere at the two stations.

Martyn (1953) has shown that the disturbance daily variation (difference between the diurnal variations on the magnetically disturbed and quiet days) of the foF2 and the minimum virtual height, h′F2, of the F2 layer depends upon the latitude of the station. There is a general tendency of the electron density to be raised at low latitudes but to be decreased at higher latitudes.

Skinner and Wright (1955) have examined in detail the differences between the magnetically quiet and disturbed day variations of the maximum electron

UNIVERSITY OF MICHIGAN LIBRARIES

density, NmF2 $\propto$ (foF2)^2, minimum virtual height, h'F2, the height of maximum ionization (hmF2) in the F2 layer at Ibadan during the year 1952. Following their criterion, the days are taken as magnetically quiet or magnetically disturbed according to the daily sum of geomagnetic planetary three-hour range indices, *i.e.*, $\Sigma K_p \leqslant 15$ or $\Sigma K_p \geqslant 31$ respectively. The average values of the ionospheric characteristics at Leopoldville for such classified groups of magnetically quiet and disturbed days are evaluated separately. The virtual height of the F2 layer at a frequency equal to 0·834 times foF2, designated by hpF2, is taken as the height of maximum ionization in the F2 layer at Leopoldville. The hpF2 is known to be very close to the hmF2 values derived by Appleton and Beynon's method (1940).

Figure 1 shows the whole year average diurnal variation of NmF2, h'F2 and hmF2 or hpF2 on the magnetically quiet and disturbed days at Ibadan and Leopoldville. The curves for Ibadan are those given by Skinner and Wright (1955). The values of NmF2 at Ibadan are distinctly greater during the disturbed than during the quiet days. But there is no significant difference between the quiet and disturbed day values of NmF2 at Leopoldville. The values of h'F2 for the daylight hours at Ibadan are decreased during the disturbed days, but there is only a slight tendency of the same at Leopoldville for a few hours around noon. The values of hmF2 at Ibadan are greater on quiet than on disturbed days for the forenoon hours, but it is otherwise for the afternoon hours. At Leopoldville, there is a tendency for the hpF2 variation to be opposite to the variation of hmF2 at Ibadan. The disturbed day values of hpF2 at Leopoldville are greater than the corresponding quiet day values for the forenoon hours, but are less during the afternoon hours.

The very little difference between the quiet and disturbed day values of NmF2 at Leopoldville could be due either to the fact that the magnetic disturbance has little effect on NmF2 at all seasons, or it may have large but opposite effects in the different seasons. Therefore, the variations of these parameters at Leopoldville are evaluated separately for the northern and southern solsticial months and are shown in Fig. 2.

One finds large differences between the quiet and disturbed day values of NmF2 during either of the seasons. The electron density, NmF2, for any hour of the day is greater on the disturbed than on the quiet days during the northern solsticial months (local winter). But, during the southern solsticial months (local summer), the values of NmF2 are much smaller on the disturbed than on the quiet days. This effect at Leopoldville is similar to that at Canberra and Watheroo as found by Martyn (1953), *i.e.*, during the magnetically disturbed days the mean values of foF2 are depressed in summer

months and are slightly raised in winter months. The disturbance daily variation of foF2 at Leopoldville (geomagnetic latitude $\phi = 3{\cdot}1°$ S, magnetic latitude $\mu = 18°$ S) thus resembles the same at Watheroo ($\phi = 41{\cdot}7°$ S, $\mu = 47°$ S) and Canberra ($\phi = 43{\cdot}8°$ S, $\mu = 47°$ S), but is very different from

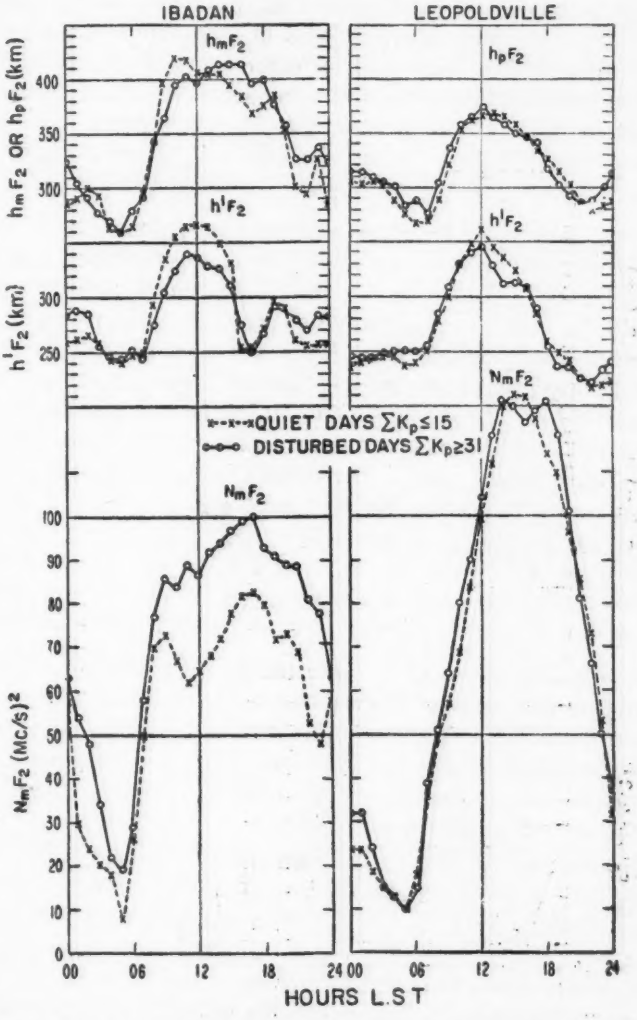

FIG. 1. The quiet and disturbed day variations of the maximum electron density (NmF2), the minimum virtual height (h'F2) and the height of the maximum ionization (hmF2 or hpF2) of the F2 layer at Ibadan and Leopoldville for the year 1952.

that of Ibadan ($\phi = 10{\cdot}6°$ N, $\mu = 2{\cdot}5°$ S). This shows the consistency of the results grouped on the basis of magnetic latitudes.

The effect of magnetic storms on the F2 layer can also be described by the storm time (Dst) variation of foF2. This is generally expressed as the variation of 200 (foF2–$\bar{f}$oF2)/foF2 with the time since the commencement of the storm, where foF2 is the value during the hours following the storm and $\bar{f}$oF2 is the monthly median value corresponding to the same local time.

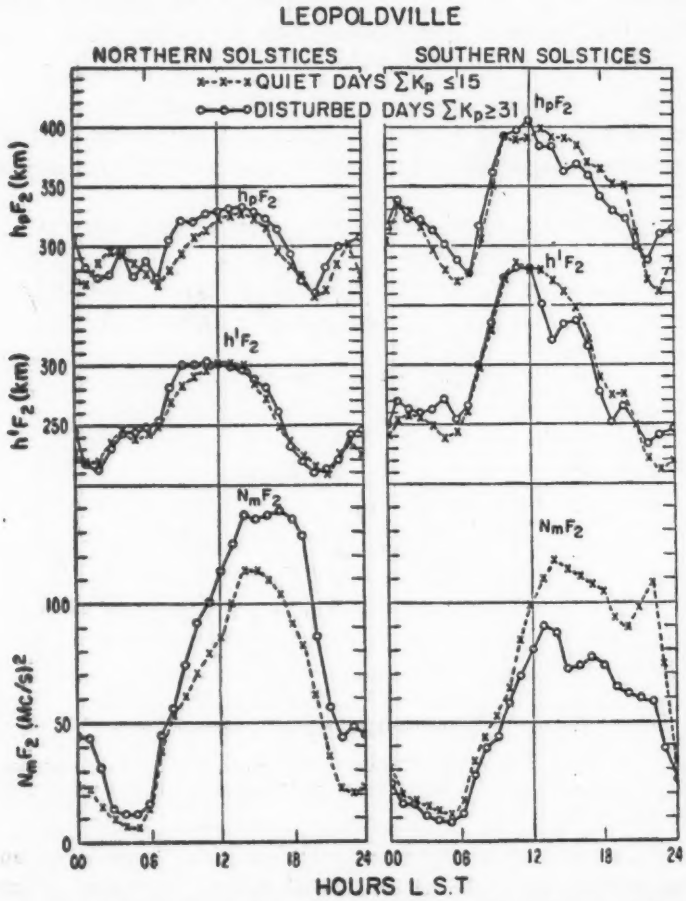

FIG. 2. The quiet and disturbed days variations of maximum electron density (NmF2), the minimum virtual height (h'F2) and the height of the maximum ionization (hpF2) of the F2 layer over Leopoldville during the northern and southern solsticial months of 1952.

This quantity approximately equals the percentage variation of the maximum electron density, NmF2, in the F2 layer. Matsushita (1959) has studied the Dst variation of foF2 at a large number of stations, which were grouped into different zones according to the geomagnetic latitude of the stations. It was stated that the Dst variations at individual stations within zones so defined were very similar to each other. At the equatorial zone within geomagnetic latitudes $\pm$ 10°, the magnetic storm is followed by a short decrease and later by an increase reaching a maximum at about 1½ days after the commencement of the storm. At higher latitudes, the magnetic storm causes an initial short increase of foF2 followed by a large decrease with a maximum at about 1½ days after the commencement of the storm.

In Fig. 3 are shown the storm time variations of foF2 at Ibadan and Leopoldville averaged for 19 strong sudden commencement type magnetic storms (maximum $A_p \geq 50$) during the period 1952–1956. The Dst variation

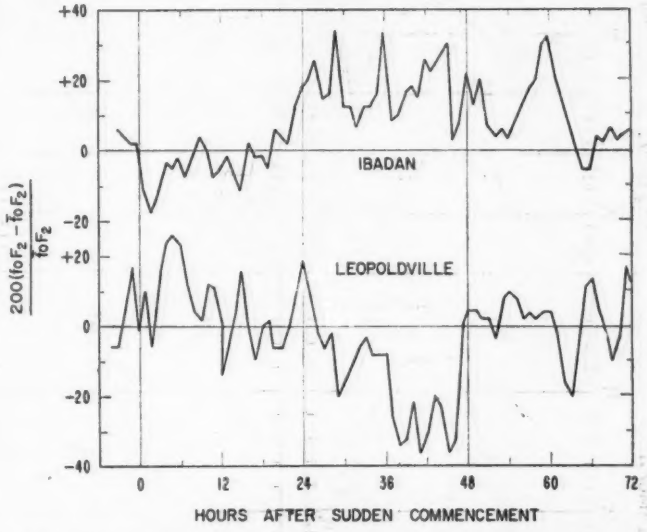

FIG. 3. The averaged percentage variation of the maximum electron density in the F2 layer at Ibadan and Leopoldville at hours following sudden commencement of magnetic storm during 1952–56.

of foF2 at Ibadan consists of a small decrease during the first day and large and consistent increases during the second day of the storm. Contrary to this, the Dst variation of foF2 at Leopoldville consists of a short increase during the first day followed by large decreases, with the minimum at about

40 hours after the commencement of the storm. The curves for the two stations are distinctly opposite in nature. The variation at Ibadan is of the equatorial type. However, the variation at Leopoldville is of the high latitude type.

It is concluded that the effect of geomagnetic activity on the variations of the F2 layer ionization at low latitudes is determined by the magnetic and not by the geomagnetic latitude of the station.

ACKNOWLEDGEMENTS

The author is deeply thankful to the High Altitude Observatory of the University of Colorado, Boulder, for awarding him a post-doctoral fellowship. Sincere thanks are also due to the National Bureau of Standards, Boulder, for giving him all facilities at their Boulder Laboratories and at the World Data Centre A.

REFERENCES

Appleton, E. V. and Beynon, W. J. G. — *Proc. Phys. Soc.*, 1940, **52**, 518.

Brown, R. A. .. *J. Atmos. Terres. Phys.*, 1956, **9**, 144.

Martyn, D. F. .. *Nature* (*London*), 1953 *a*, **171**, 14.

——— .. *Proc. Roy. Soc.*, 1953 *b*, **218 A**, 1.

Matsushita, S. .. *J. Geophys. Res.*, 1959, **64**, 305.

Rastogi, R. G. .. *Canadian S. Phys.*, 1959, **37**, 274.

——— .. *J. Atmos. Terres. Phys.*, 1960, **18**, 315.

——— .. *Nature* (*London*), 1961, **189**, 214.

Skinner, N. J. and Wright, R. W. *J. Atmos. Terres. Phys.*, 1955, **6**, 177.

HETEROCYCLIC COMPOUNDS

Part XVII.* Synthesis of Dihydrofuro (2′: 3′—2 : 3) Quinoline

By Joseph P. John and P. Shanmugam

(*Department of Organic Chemistry, University of Madras, Madras-25*)

Received August 1, 1961

(Communicated by Dr. K. N. Menon, F.A.SC.§)

Furo-(2′: 3′–2: 3) quinoline ring system is present in many alkaloids of the Rutaceæ family. Synthesis of dihydrofuro-(2′: 3′–2: 3) quinolines, starting from *o*-amino ketones and aldehydes has been described in the previous paper.[1] The amino ketone or the aldehyde is treated with succinic anhydride in hot benzene. The succinoyl derivative, which separates on cooling, is then cyclised, by refluxing with 2% aqueous potassium hydroxide. The ester of the quinolone acid (II), thus obtained, is reduced to the alcohol (III), which is then ring closed to the dihydro-furo-quinoline (IV). This paper describes the synthesis of dihydro-furo (2′: 3′–2: 3) quinoline and its 6: 7-methylene-dioxy analogue (VIII). The infra-red spectra of both the bases show fairly intense absorption in 1639^{-1} cm. region.

Kobashi and Kurvayama[4] obtained the base (IV) by heating 4, 5-dihydro-3-furanilide with 85% phosphoric acid at 150–60° for 8 hours.

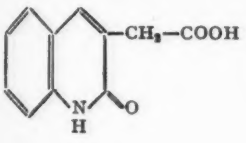

I

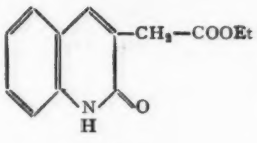

II

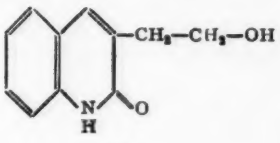

III

IV

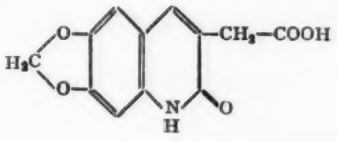

V

* Part XVI, *Proceedings*, 1960, **51 A** (2).

§ Present address: Panthyil House, Warriam Road, Ernakulam (Kerala).

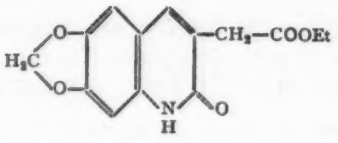

VI

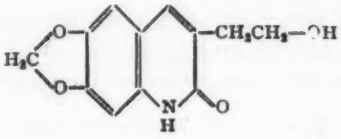

VII

VIII

EXPERIMENTAL

(*a*) 4′ : 5′-*dihydrofuro* (2′ : 3′–2 : 3) *quinoline* (*IV*)

2-*Quinolone*-3-*acetic acid* (*I*).—*o*-Aminobenzaldehyde[2] (3 g.) and succinic anhydride (2·5 g.) were heated together in boiling benzene for 30 minutes. The succinoyl derivative that separated on cooling was collected and refluxed with 2% aqueous potassium hydroxide (250 ml.) for one hour. The solution was cooled and acidified with hydrochloric acid when the quinolone acid separated. It was collected, washed with water and then with little alcohol. It crystallised from acetic acid in needles, m.p. 277–78° C. (dec.).

Found: C, 64·9; H, 4·2. $C_{11}H_9NO_3$ requires: C, 65·01; H. 4·45.

Ethyl-2 *quinolone*-3 *acetate* (*II*).—The above acid (3 g.) was refluxed with absolute ethanol (50 ml.) containing concentrate sulphuric acid (1·5 ml.) for 5 hours. The product was collected after dilution with ice-water, and crystallised from alcohol in needles, m.p. 186–87° C.

Found: C, 67·5; H, 5·05. $C_{13}H_{13}NO_3$ requires: C, 67·53; H, 5·63.

3-(2′-*hydroxyethyl*)-2-*quinolone* (III).—The above ester (1 g.) was reduced with lithium aluminium hydride (0·5 g.) in tetrahydrofuran, and the product isolated as described previously.[1] It crystallised from benzene in colourless needles, m.p. 196° C.

Found: C, 69·21; H, 5·7. $C_{11}H_{11}NO_2$ requires: C, 69·8; H 5·8.

4′ : 5′-*dihydrofuro* (2′ : 3′–2 : 3) *quinoline* (*IV*).—The above alcohol (0·5 g.) was heated with polyphosphoric acid (from 5 g. of P_2O_5 and 3 ml. of phosphoric acid) for 4 hours on a steam-bath. After cooling the viscous product was poured into ice-water, basified with ammonia and extracted with chloroform. The solvent was evaporated and the residue dissolved in dry benzene

and passed through a column of alumina. The benzene was removed and the dihydro-furo quinoline was obtained as colourless plates. It crystallised from petroleum ether in colourless plates, m.p. 121–22° C. I.R. 1639 $cm.^{-1}$

Found: C, 76·89; H, 5·10. $C_{11}H_9NO$ requires: C, 77·2; H, 5·26.

(*b*) 6:7-*Methylenedioxy-4':5'-dihydrofuro* (2', 3'–2:3) *quinoline.*

6:7-*Methylenedioxy-2-quinolone-3-acetic acid* (*V*).—6-Aminopiperonal[3] (5 g.) was heated with succinic anhydride (3·5 g.) in boiling benzene for 30 minutes, cooled and the succinoyl derivative was collected and washed with little benzene. It was refluxed with 2% aqueous potassium hydroxide (350 ml.) for 1 hour. After cooling it was extracted with benzene to remove the free amino-aldehyde. The aqueous layer on acidification furnished the quinolone acetic acid. Crystallised from acetic acid, m.p. 290–92° C. (dec.).

Found: C, 58·33; H, 4·1. $C_{12}H_9NO_5$ requires: C, 58·3; H, 3·64.

Ethyl-6:7-*methylenedioxy-2-quinolone-3-acetate* (*VI*).—The above acid (3 g.) was suspended in absolute ethanol (100 ml.) and saturated with dry hydrogen chloride at 0·5° C. It was kept at room temperature for 24 hours. The product, after dilution with water, was collected and crystallised from ethanol, m.p. 235–36° C.

Found: C, 61·08; H, 4·73. $C_{14}H_{13}NO_5$ requires: C, 61·09; H, 4·73.

3-(2'-*hydroxyethyl*)-6:7-*methylenedioxy-2-quinolone* (*VII*).—The above ester (1 g.) was reduced with lithium aluminium hydride (0·5 g.) in tetrahydrofuran and the product isolated as in the previous case. Crystallised from alcohol, m.p. 243–44° C.

Found: C, 61·71; H, 4·65. $C_{12}H_{11}NO_4$ requires: C, 61·8; H, 4·72.

6:7-*Methylenedioxy-4':5'-dihydrofuro* (2':3'–2:3)-*quinoline* (*VIII*).—The alcohol (1 g.) was heated with polyphosphoric acid, on a steam-bath for 4 hours. After cooling the viscous reaction mixture was poured into ice-water and basified with ammonia. The product separated in fine needles. Crystallised from alcohol, m.p. 188–89° C.

Found: C, 67·61; H, 4·30. $C_{12}H_9NO_3$ requires; C, 66·99; H, 4·18. I.R. 1639^{-1} cm.

ACKNOWLEDGEMENT

We thank Dr. K. N. Menon, Professor of Organic Chemistry, University of Madras, for his help and the Government of India for a Senior Research Scholarship to one of us (J.P.J.).

REFERENCES

1. Shanmugam, P. .. *Proc. Ind. Acad. Sci.*, 1960, **51**, 75–83.
2. Smith, L. T. and Opic, J. W. *Org. Synth.*, **28**, 11.
3. Campbell, Hooper and Campbell *J. Org. Chem.*, 1951, **16**, 1740–41.
4. Kobashi and Kurvayama .. *J. Pharm. Soc. Japan*, 1959, **79**, 124, (*C.A.*, 1959, 1022–23).

HETEROCYCLIC COMPOUNDS

Part XVIII.* Synthetic Experiments in the Quinazoline Series

By M. Krishnan‡

(Department of Organic Chemistry, University of Madras, Madras-25)

Received August 1, 1961

(Communicated by Dr. K. N. Menon, F.A.SC.)

The attempted synthesis of 2-methyl-4-benzylquinazoline resulted in the formation of 2-methyl-4-benzoylquinazoline due to facile oxidation of the methylene group.[1] It would be interesting to study the reactions with substituted 4-benzylquinazolines with a view of studying the effect of substituents on the rate of oxidation of the 4-benzyl portion of quinazolines. However, this would necessitate as starting intermediates with substituents in the 3-benzyl position. Such compounds are defficultly accessible. So it was decided to study the formation of various substituted 2-benzylquinazolines and to study their behaviour with respect to their susceptibility to air oxidation.

The work presented in this paper relates to the preparation of 4-methyl-2-benzylquinazolines with substituents both in the benzene part and 2-benzyl part of quinazoline. The following scheme of reactions for the syntheses of different substituted 2-benzylquinazolines was based on the method of Bishler *et al.*[2, 3]

2-Nitro-3 : 4-dimethoxyacetophenone required for the synthesis of 4-methyl-2-benzyl-7 : 8-dimethoxyquinazoline (III, $R = R_3 = R_4 = H$; $R_1 = R_2 = OCH_3$) was prepared. 2-Nitroveratroyl chloride was condensed with the magnesium ethoxy derivative of diethyl malonate in benzene to yield 2-nitroveratroyl diethylmalonate. The oily acyl malonate on refluxing with propionic acid for three hours underwent hydrolysis and decarboxylation to 2-nitro-3 : 4-dimethoxyacetophenone. The reduction of the nitroketone to aminoketone was carried out with iron powder and glacial acetic acid. The cyclisation of 2-phenylacetamido-3 : 4-dimethoxyacetophenone (II, $R = R_3 = R_4 = H$; $R_1 = R_2 = OCH_3$) to the corresponding quinazoline

---

* Part XVII, *Proceedings*.

‡ Present Address: Senior Research Fellow, Shri Ram Institute for Industrial Research, Delhi-8.

was effected by means of ammonia. Similarly, 4-methyl-2-benzyl-6:7-dimethoxyquinazoline (III, $R = R_1 = OCH_3$; $R_2 = R_3 = R_4 = H$) and 4-methyl-2-benzyl-7-methoxyquinazoline (III, $R_1 = OCH_3$; $R = R_2 R_3 = R_4 = H$) were prepared in a similar manner starting from 2-amino-4:5-dimethoxyacetophenone and 2-amino-4-methoxyacetophenone respectively. *m*-Nitrophenylacetyl chloride, *o*-methoxyphenylacetyl chloride, *o*-tolylacetyl chloride and *m*-tolylacetyl chloride were condensed with *o*-aminoacetophenone and the phenylacetamides were cyclised to the corresponding 2 : 4-disubstituted quinazolines by means of ammonia.

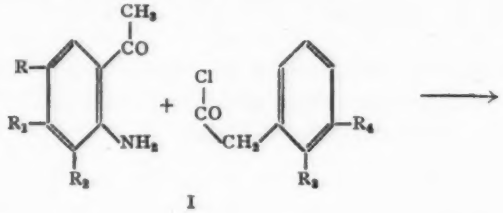

I

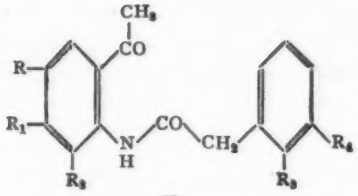

II

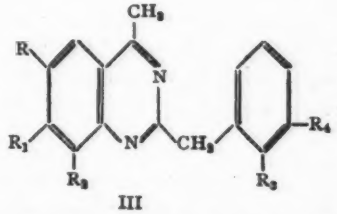

III

The substituted benzylquinazoline was dissolved in alcohol and the solution was either exposed to air for several days or air was bubbled through the solution for several hours, keeping the volume of the solution constant. In all cases the starting materials were recovered unchanged indicating that no oxidation took place.

EXPERIMENTAL

(1) *4-Methyl-2-benzyl-7 : 8-dimethoxyquinazoline* (*III*, $R = R_3 = R_4 = H$; $R_1 = R_2 = OCH_3$)

2-Nitro-3 : 4-dimethoxyacetophenone.—A benzene solution of the magnesium ethoxy derivative of diethyl malonate (24 g.) was prepared from 3·6 g. of Grignard magnesium and 10 c.c. of absolute ethanol by standard procedure. 2-Nitroveratric acid, prepared according to the method of Pschorr and Somuleau,[4] was converted into the acid chloride. A slightly more than equivalent quantity of 2-nitroveratroyl chloride (24 g.) in benzene (75 c.c.) was added to a cooled solution of the prepared magnesium

derivative of diethyl malonate during 30 mins. After completion of addition, the mixture was refluxed for 1 hour and left to stand overnight. The magnesium complex was decomposed with dilute acid and the acid layer was extracted with benzene. The organic layer was dried and solvent removed. The crude acyl malonate was obtained as an oil.

The acyl malonate (35 g.), propionic acid (60 g.) and conc. sulphuric acid (1·8 g.) were refluxed for three hours. When the evolution of carbon dioxide stopped, more of sulphuric acid (20 c.c. of 4 N) was added and the refluxing was continued for three more hours. The solution was poured into water and left overnight. The solid was collected and crystallised from alcohol. Yield 15 g.; m.p. 91–92° C. Found: C, 53·7; H, 4·83; $C_{10}H_{11}NO_5$ requires C, 53·33; H, 4·88. The 2:4-dinitrophenylhydrazone crystallised as orange crystals from glacial acetic acid, m.p. 235° C. Found: N, 17·00; $C_{16}H_{15}O_5N_5$ requires N, 17·28.

2-*Amino*-3 : 4-*dimethoxyacetophenone*.—2-Nitro-3 : 4-dimethoxyacetophenone (7 g.) was dissolved in glacial acetic acid (50 c.c.) and iron filings (7·5 g.) were added during one hour at the temperature of water-bath. After reduction, the amino-ketone was isolated in the usual manner and was crystallised from light petrol, when a white crystalline product (5 g.) of m.p. 89–90° C. was obtained. Found: N, 7·5; $C_{10}H_1N_3O_3$ requires N, 7·2.

2-*Phenylacetamido*-3: 4-*dimethoxyacetophenone* (*II*, $R = R_3 = R_4 = H$; $R_1 = R_2 = OCH_3$).—This was prepared by the reaction of phenylacetyl chloride with the above amino-ketone. The amide was crystallised from benzene and petroleum ether, m.p. 115° C. Found: N, 4·85; $C_{18}H_{19}NO_4$ requires N, 4·5.

4-*Methyl*-2-*benzyl*-7 : 8-*dimethoxyquinazoline* (*III*, $R = R_3 = R_4 = H$; $R_1 = R_2 = OCH_3$).—The foregoing amide (1·5 g.) was mixed with dry ammonium acetate (15 g.) and dry ammonia was passed continuously through the molten solution kept at 165° C. for 4 hours. It was then cooled and poured into water. The aqueous solution was repeatedly extracted with solvent and the extract washed with dilute acid. Basification of the acid extract yielded the base. The quinazoline was crystallised from dilute alcohol, m.p. 147–48° C. Found: N, 9·8; $C_{18}H_{18}N_2O_2$ requires N, 9·6.

(2) 4-*Methyl*-2-*benzyl*-7-*methoxyquinazoline* (*III*, $R = R_2 = R_3 = R_4 = H$; $R_1 = OCH_3$)

2-*Nitro*-4-*methoxyacetophenone*.—This was prepared from 2-nitro-4-methoxy-benzoyl chloride and diethyl malonate.[5] Its 2:4-dinitophenyl-

hydrazone formed red crystals from glacial acetic acid, m.p. 225° C. Found: C, 47·59; H, 3·0; $C_{15}H_{13}N_5O_7$ requires C, 47·89; H, 3·4.

2-Phenylacetamido-4-methoxyacetophenone (*II*, $R = R_2 = R_3 = R_4 = H$; $R_1 = OCH_3$).—Treatment of phenylacetyl chloride (3·8 g.) with 2-amino-4-methoxyacetophenone[5] (4·1 g.) in the presence of pyridine yielded 2-phenylacetamido-4-methoxyacetophenone of m.p. 92–94° C. Recrystallisation from alcohol yielded brown granular substance of m.p. 96–97° C. Found: C, 72·4; H, 6·1; $C_{17}H_{17}O_3N$ requires C, 72·6; H, 6·2.

4-Methyl-2-benzyl-7-methoxyquinazoline (*III*, $R = R_2 = R_3 = R_4 = H$; $R_1 = OCH_3$).—The above amide (2 g.) was cyclised to the base in the same manner as described before. The base (1·1 g.) was found to be quite soluble in organic solvents. Analytical sample was prepared from dil. alcohol, m.p. 100° C. Found: N, 10·4; $C_{17}H_{16}N_2O$ requires N, 10·6.

(3) *4-Methyl-2-benzyl-6: 7-dimethoxyquinazoline* (*III*, $R = R_1 = OCH_3$; $R_2 = R_3 = R_4 = H$)

2-Nitro-4: 5-dimethoxyacetophenone.—The above ketone was prepared from 6-nitroveratroyl chloride and diethyl malonate in an analogous manner as described for 2-nitro-3: 4-dimethoxyacetophenone. The yields were good when compared to the previous method of preparation. 6-Amino-veratrophenone was obtained by the reduction of the above nitro ketone.[6]

2-Phenylacetamido-4 : 5-dimethoxyacetophenone (*II*, $R = R_1 = OCH_3$; $R_2 = R_3 = R_4 = H$).—2-Amino-4: 5-dimethoxyacetophenone was converted into the phenylacetyl derivative. The amide was crystallised from benzene and petroleum ether, m.p. 138–39° C. Found: N, 4·8; $C_{18}H_{19}NO_4$ requires N, 4·5.

4-Methyl-2-benzyl-6: 7-dimethoxyquinazoline (*III*, $R = R_1 = OCH_3$; $R_2 = R_3 = R_4 = H$).—The above amide (3 g.) was cyclised by ammonia. The base (2 g.) was crystallised from light petrol, m.p. 140–41° C. Found: N, 9·8; $C_{18}H_{18}N_2O_2$ requires N, 9·52.

(4) *4-Methyl-2-(m-nitrobenzyl) quinazoline* (*III*, $R = R_1 = R_2 = R_3 = H$; $R_4 = NO_2$)

2-(m-Nitrophenylacetamido)-acetophenone (*II*, $R = R_1 = R_2 = R_3 = H$; $R_4 = NO_2$).—*m*-Nitro-phenylacetyl chloride (5 g.) and *o*-aminoacetophenone were condensed to yield the above amide. Recrystallisation from methanol afforded white needles, m.p. 120–21° C. Found: N, 9·26; $C_{16}H_{14}N_2O_4$ requires N, 9·39.

4-*Methyl*-2-(m-*nitrobenzyl*) *quinazoline* (*III*, $R = R_1 = R_2 = R_3 = H$; $R_4 = NO_2$).—The amide was cyclised to the base by means of ammonia. The base was obtained as yellow needles from methyl aclohol, m.p. 132° C. Found: N, 14·7; $C_{16}H_{13}N_3O_3$ requires N, 15·0.

(5) 4-*Methyl*-2-(o-*methylbenzyl*)-*quinazoline* (*III*, $R = R_1 = R_2 = R_4 = H$; $R_3 = CH_3$)

2-(o-*Tolylacetamido*) *acetophenone* (*II*, $R = R_1 = R_2 = R_4 = H$; $R_3 = CH_3$).—*o*-Methylphenylacetyl chloride was condensed with *o*-aminoacetophenone in the presence of pyridine to yield the amide. Yellow crystals were obtained on recrystallisation from alcohol, m.p. 69° C. Found: N, 5·8; $C_{17}H_{17}NO$ requires N, 5·57.

4-*Methyl*-2-(o-*methylbenzyl*) *quinazoline* (*III*, $R = R_1 = R_2 = R_4 = H$; $R_3 = CH_3$).—The above base was prepared by the cyclisation of the foregoing amide. White needles of m.p. 59–60° C. were obtained. The base was found to be very soluble in alcohol, chloroform and other organic solvents. Found: N, 11·5; $C_{17}H_{16}N_2$ requires N, 11·29.

(6) 4-*Methyl*-2-(m-*methylbenzyl*)-*quinazoline* (*III*, $R = R_1 = R_2 = R_3 = H$; $R_4 = CH_3$)

2-(*m*-Tolylacetamido)-acetophenone obtained by the condensation of *m*-methylphenylacetyl chloride and *o*-aminoacetophenone was straightaway used for the cyclisation. The amide was cyclised to the base by procedures adopted for the similar cyclisations. The base was obtained as a low melting solid and purification proved difficult. So 4-methyl-2-(*m*-methylbenzyl)-quinazoline was converted into picrate and analysed. The picrate was crystallised from dilute methanol, m.p. 181° C. Found: N, 14·2; $C_{23}H_{19}N_5O_7$ requires N, 14·6.

(7) 4-*Methyl*-2-(o-*methoxybenzyl*)-*quinazoline* (*III*, $R = R_1 = R_2 = R_4 = H$; $R_3 = OCH_3$)

2-(o-*Methoxyphenylacetamido*)-*acetophenone* (*II*, $R = R_1 = R_2 = R_4 = H$; $R_3 = OCH_3$).—The amide was obtained in the usual manner by the condensation of 4·5 g. of *o*-aminoacetophenone and 5·5 g. of *o*-methoxyphenylacetyl chloride in the presence of pyridine. The amide was crystallised from methanol; yellow crystals, m.p. 97–98° C., were obtained. Found: N, 5·15; $C_{17}H_{17}NO_3$ requires N, 4·95.

4-*Methyl*-2-(o-*methoxybenzyl*)-*quinazoline* (*III*, $R = R_1 = R_2 = R_4 = H$; $R_3 = OCH_3$).—The above amide (3 g.) was cyclised by ammonia in the presence

of dry ammonium acetate. Working up the product in the same way, the base was obtained as a yellow crystalline substance. It was crystallised from light petrol; yellow crystals, m.p. 92-93° C. Found: N, 10·77; $C_{17}H_{16}N_2O$ requires N, 10·6.

SUMMARY

The synthesis of substituted 2-benzylquinazolines is reported.

ACKNOWLEDGEMENT

The author is thankful to Dr. K. N. Menon for his help and guidance during the course of this work.

REFERENCES

1. Krishnan .. *Proc. Ind. Acad. Sci.*, 1958, **47**, 98.
2. Bishler and Lang .. *Ber.*, 1895, **28**, 279.
3. ——— and Howel .. *Ibid.*, 1893, **26**, 1384.
4. Pschorr and Somuleau .. *Ibid.*, 1899, **32**, 3405.
5. Schofield and Osborn .. *J. Chem. Soc.*, 1955, 2103.
6. Simpson .. *Ibid.*, 1946, 95.
7. Castle and Kruse .. *J. Org. Chem.*, 1952, **17 A**, 1571.

AN APPROXIMATE METHOD FOR THE CALCULATION OF THE INCOMPRESSIBLE LAMINAR SPANWISE BOUNDARY LAYER ON AN INFINITE UNIFORM YAWED CYLINDER WITH DISTRIBUTED SUCTION

By Dr. Kapildeo Prasad Sinha

(Mathematics Department, Science College, Patna)

Received September 7, 1960

(Communicated by Dr. N. S. Nagendra Nath, F.A.Sc., F.N.I.)

Abstract

This paper describes an approximate method to calculate the incompressible laminar spanwise boundary layer on an infinite yawed uniform cylinder with distributed suction. The calculation for the chordwise layer is supposed to be known. A similar method to calculate the laminar spanwise layer for a solid boundary is given by Rott and Crabtree, but for a porous boundary with suction no such method is known to the author at present except the one given in this paper. The present method is equally applicable to a solid boundary also. A comparison of the calculation by the present approximate method is made with the exact solutions of the spanwise layer with the chordwise velocity distribution $U = Cx^m$ at the edge of the layer, and the agreement is found to be quite satisfactory. Moreover, the method is very simple in operation.

1. Introduction and Summary

This paper describes an approximate method to calculate the incompressible laminar spanwise boundary layer on an infinite yawed uniform cylinder with distributed suction. The calculation for the chordwise layer is supposed to be known. A similar method to calculate the laminar spanwise layer for a solid boundary is given by Rott and Crabtree,[1] but for a porous boundary with suction no such method is known to the author at present except the one given in this paper. The present method is equally applicable to a solid boundary also. A comparison of the calculation by the present approximate method is made with the exact solutions of the spanwise layer with the chordwise velocity distribution $U = Cx^m$ at the edge of the layer, and the agreement is found to be quite satisfactory. Moreover, the method is very simple in operation.

2. NOTATION

x, y, z = Co-ordinates measured in the tangential direction, spanwise direction and normal to the surface respectively (Fig. 1).

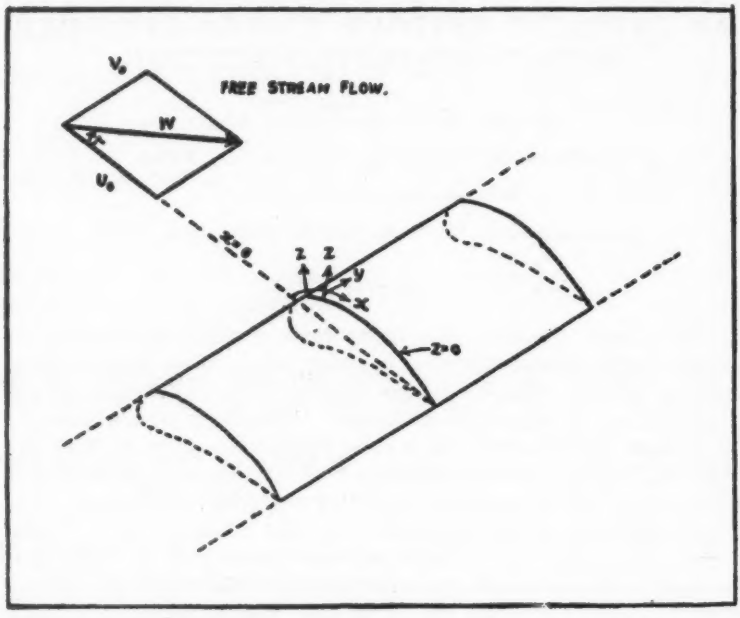

FIG. 1. Sketch showing the orthogonal curvilinear co-ordinates for the flow past an infinite yawed, uniform cylinder.

u, v, w = Velocity components in the boundary layer in x, y and z directions respectively.

U = Chordwise velocity at the edge of the boundary layer.

C = A constant in the expression $U = Cx^m$.

m = Index in the relation $U = Cx^m$.

V_0 = Spanwise component in the free stream.

p = Static pressure in the boundary layer.

U^1 = $\frac{dU}{dx}$.

w_0 = Normal suction velocity at the surface.

μ = Coefficient of viscosity.

ρ = Density of the air.

$\nu = \dfrac{\mu}{\rho}$ = Kinematic viscosity.

$\delta_x^* = \int_0^\infty \left(1 - \dfrac{u}{U}\right) dz$ = displacement thickness for the chordwise layer.

$\theta_x = \int_0^\infty \dfrac{u}{U}\left(1 - \dfrac{u}{U}\right) dz$ = momentum thickness of the chordwise layer.

$\delta_y^* = \int_0^\infty \left(1 - \dfrac{v}{V_0}\right) dz$ = displacement thickness for the spanwise layer.

$\theta_y = \int_0^\infty \dfrac{v}{V_0}\left(1 - \dfrac{v}{V_0}\right) dz$ = momentum thickness for the spanwise layer.

$H_x = \dfrac{\delta_x^*}{\theta_x}$ = shape factor for the chordwise profile in the boundary layer.

$H_y = \dfrac{\delta_y^*}{\theta_y}$ = shape factor for the spanwise profile in the boundary layer.

$\theta_{xy} = \int_0^\infty \dfrac{u}{U}\left(1 - \dfrac{v}{V_0}\right) dz$ = mixed momentum thickness of the boundary layer.

a_y = a parameter for the family of spanwise profiles.

$l_y = \dfrac{\theta_y}{V_0}\left(\dfrac{\partial v}{\partial z}\right)_{z=0}$ = non-dimensional skin-friction parameter for the spanwise boundary layer.

$m_y = \dfrac{\theta_y^2}{V_0}\left(\dfrac{\partial^2 v}{\partial z^2}\right)_{z=0}$ = a shape parameter for the spanwise profile.

$s = \dfrac{\theta_{xy}}{\theta_x}$ = ratio of the mixed momentum thickness to the chordwise momentum thickness.

$q = \frac{\theta_y}{\theta_x}$ = ratio of the momentum thickness of the boundary layer in the spanwise and chordwise directions.

$\lambda_x = \frac{-w_0\theta_x}{\nu}$ = a suction parameter for the chordwise boundary layer.

$\lambda_y = \frac{-w_0\theta_y}{\nu}$ = a suction parameter for the spanwise boundary layer.

$\xi = \frac{z}{\theta_x}$ = a non-dimensional variable.

δ_x = a measure of the chordwise boundary layer thickness.

δ_y = a measure of the spanwise boundary layer thickness.

$\eta_x = \frac{z}{\delta_x}$ = a non-dimensional variable in the chordwise profile.

K_x = form parameter for the chordwise profile.

$\eta_y = \frac{z}{\delta_y}$ = a non-dimensional variable in the spanwise profile.

K_y = form parameter for the spanwise profile.

$\gamma = \frac{\delta_y}{\delta_x}$ = ratio of the measure of the spanwise boundary layer thickness to that of the chordwise boundary layer thickness.

$g_x = \frac{\theta_x}{\delta_x}$ = ratio of the chordwise momentum thickness to the measure of the chordwise boundary layer thickness.

$g_y = \frac{\theta_y}{\delta_y}$ = ratio of the spanwise momentum thickness to the measure of the spanwise boundary layer thickness.

$g_{xy} = \dfrac{\theta_{xy}}{\delta_y}$ = ratio of the mixed momentum thickness to the measure of the spanwise boundary layer thickness.

$\left.\begin{matrix} a_\nu \\ b_\nu \end{matrix}\right\}\ \nu = 0, 1, 2, 3$ = coefficients in the expressions for g_{xy}.

H_t = a variable to denote H_x or H_y in equation (33).

K_t = a variable to denote K_x or K_y in equation (33).

3. Outline and Development of the Method

There are three important steps in the construction of this method. The first is to recast the mixed momentum equation in a form which is convenient for step-by-step computation. The second step is the construction of curves or numerical tables for s and q in terms of H_x and H_y, which respectively determine the shapes of the chordwise and spanwise velocity profiles. This numerical relation between s and q is evaluated by using a family of approximate velocity profiles introduced by Schlichting[2] for the chordwise and spanwise layers. The third step is to simplify the calculation of H_y by using Iglisch's solution[3] on a flat plate with constant suction. The basic assumption underlying the first and the third steps is that the spanwise profiles are approximately a function of suction only on (z/θ_y) scale. This assumption was suggested by the results obtained by the present author.[4]

3.1. *Simplification in the mixed momentum equation*

The boundary layer equation for the incompressible laminar flow over an infinite yawed uniform cylinder are

$$u\frac{\partial u}{\partial x} + w\frac{\partial u}{\partial z} = -\frac{1}{\rho}\frac{\partial p}{\partial x} + \nu\frac{\partial^2 u}{\partial z^2} \tag{1}$$

$$u\frac{\partial v}{\partial x} + w\frac{\partial v}{\partial z} = \nu\frac{\partial^2 v}{\partial z^2} \tag{2}$$

$$\frac{\partial p}{\partial z} = 0 \tag{3}$$

and the equation of continuity is

$$\frac{\partial u}{\partial x} + \frac{\partial w}{\partial z} = 0. \tag{4}$$

The boundary conditions are:

(*a*) at the surface $z = 0$, $u = v = 0$ and $w = w_0$ is zero or non-zero according as the boundary is solid or porous, and (*b*) at the edge of the boundary layer

$$z \to \infty, \quad u = \mathrm{U}, \quad v = \mathrm{V},$$

and

$$\frac{\partial u}{\partial z} = \frac{\partial v}{\partial z} = \frac{\partial^2 u}{\partial z^2} = \frac{\partial^2 v}{\partial z^2} = 0.$$

If the flow outside the boundary layer is irrotational

$$\frac{\partial \mathrm{U}}{\partial y} - \frac{\partial \mathrm{V}}{\partial x} = 0. \tag{5}$$

Since the cylinder is infinite in length, $\partial \mathrm{U}/\partial_y = 0$, so that $v =$ constant $= \mathrm{V}_0$ (say). Also, using equation (3) and the boundary condition at the edge of the layer, equation (1) gives

$$\mathrm{U}\frac{d\mathrm{U}}{dx} = -\frac{1}{\rho}\frac{\partial p}{\partial x}. \tag{6}$$

The method really starts from the mixed momentum equation

$$\frac{d}{dx}\left\{\int_0^\infty u(\mathrm{V}_0 - v)\,dz\right\} = \nu\left(\frac{\partial v}{\partial z}\right)_{z=0} + w_0\mathrm{V}_0 \tag{7}$$

which is obtained by integrating the spanwise layer equation (2) for a porous boundary with suction. Introduce the mixed momentum thickness

$$\theta_{xy} = \int_0^\infty \frac{u}{\mathrm{U}}\left(1 - \frac{v}{\mathrm{V}_0}\right)dz \tag{8}$$

and the equation (7) reduces to

$$\frac{d}{dx}(\mathrm{U}\theta_{xy}) = \frac{\nu}{\mathrm{V}_0}\left(\frac{\partial v}{\partial z}\right)_{z=0} + w_0. \tag{9}$$

In case of suction there are two arbitrary distributions:—the pressure gradient and the suction. As mentioned before in Section 3.0, the spanwise profiles on (z/θ_y) scale will be taken as functions of suction only. Thus a spanwise profile is given by

$$\frac{v}{\mathrm{V}_0} = \mathrm{F}\left(\frac{z}{\theta_y},\ a_y\right),$$

$$= l_y(a_y)\frac{z}{\theta_y} + \frac{1}{\angle^2}m_y\left(\frac{z}{\theta_y}\right)^2 + \cdots, \tag{10}$$

where a_y depends on suction only and consequently so do l_y and m_y.

The slope of the velocity profile at the wall is given by

$$\frac{1}{V_0}\left(\frac{\partial v}{\partial z}\right)_{z=0} = \frac{l_y}{\theta_y}, \tag{11}$$

which transforms equation (9) into

$$\frac{\theta_y}{\nu}\frac{d}{dx}(U\theta_{xy}) = l_y - \lambda_y, \tag{12}$$

where

$$\lambda_y = -\frac{w_0\theta_y}{\nu}.$$

The boundary condition of the spanwise layer equation (2) on the porous wall gives

$$\lambda_y = -\frac{m_y}{l_y}, \tag{13}$$

which is also a function of suction only.

Let us define

$$s = \frac{\theta_{xy}}{\theta_x} \quad \text{and} \quad q = \frac{\theta_y}{\theta_x},$$

and then equation (12) becomes

$$\frac{d}{dx}(sU\theta_x) = \frac{\nu(l_y - \lambda_y)}{q\theta_x}. \tag{14}$$

To find the functional relationship between l_y and λ_y, Iglishch's solution[3] for a flat plate with constnat suction is used. The curves of l_y against λ_y is shown in Fig. 2. The values of l_y calculated from the exact solutions obtained by the present author[4] for the potential velocity distribution $U = Cx^m$ are also shown and they lie approximately on the same curve. The polynomial given by Thwaites[5] for this curve is

$$l_y = 0{\cdot}225 + 0{\cdot}36\lambda_y + 0{\cdot}38\lambda_y^2, \tag{15}$$

which transforms the equation (14) into

$$\frac{d}{dx}(sU\theta_x) = \frac{\nu(0{\cdot}225 - 0{\cdot}64\lambda_y + 0{\cdot}38\lambda_y^2)}{q\theta_x}. \tag{16}$$

This equation for a solid boundary becomes (putting $\lambda_y = 0$)

$$\frac{d}{dx}(sU\theta_x) = \frac{\nu\, 0{\cdot}225}{q\theta_x}, \tag{17}$$

which is the same as obtained by Rott and Crabtree.[1]

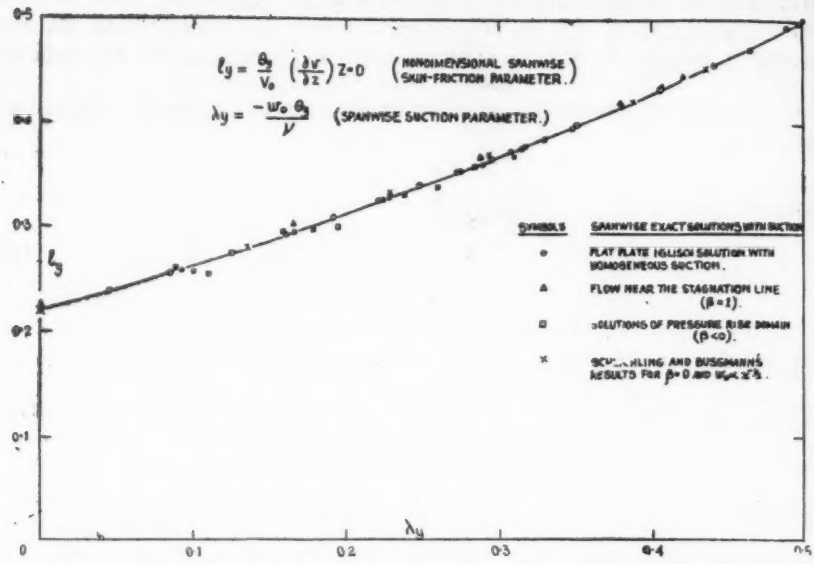

FIG. 2. Variation of l_y with γ_y based on some exact solutions of the spanwise boundary-layer with suction.

It appears that equation (16) is not sufficient to yield the characteristics of the spanwise layer, since s, q and λ_y are all unknown. Since $\lambda_y = q\lambda_x$ where λ_x is given from the chordwise layer, only a relationship between s and q is required for the solution.

3.2. *A universal relationship between* s *and* q

In the case of a solid boundary it was analytically shown by Rott and Crabtree[1] that s is a universal function of q and m_x. This was deduced on the basis that chordwise profile can be represented by a function

$$\frac{u}{U} = f\left(\frac{z}{\theta_x},\ m_x\right), \tag{18}$$

where m_x represents the shape of the profile. The spanwise profile was of fixed Blasius profile shape and was given by

$$\frac{v}{V_0} = g\left(\frac{z}{\theta_y},\ m_y = 0\right). \tag{19}$$

When suction is applied the shape of the chordwise profile is determined by both the pressure gradient and suction and that of the spanwise profile is a function of suction only. In the presence of suction, boundary

layer profiles are not immediately determined by m_x and m_y, and therefore the shape factors H_x and H_y are chosen to define the chordwise and spanwise profiles respectively. Lin[6] (p. 95) also used this parameter for this purpose.

Thus the chordwise and spanwise profiles can be represented respectively by

$$\left.\begin{aligned} \frac{u}{U} &= f\left(\frac{z}{\theta_x},\ H_x\right) \\ \text{and} \\ \frac{v}{V_0} &= g\left(\frac{z}{\theta_y},\ H_y\right) \end{aligned}\right\}. \tag{20}$$

The mixed momentum thickness in this case is

$$\theta_{xy} = \int_0^\infty f\left(\frac{z}{\theta_x},\ H_x\right)\left[1 - g\left(\frac{z}{\theta_y},\ H_y\right)\right] dz,$$

which in terms of s and q and new variable $\xi = (z/\theta_x)$ becomes

$$\begin{aligned} s &= \int_0^\infty f(\xi,\ H_x)\left[1 - g\left(\frac{\xi}{q},\ H_y\right)\right] d\xi, \\ &= s(q,\ H_x,\ H_y). \end{aligned} \tag{21}$$

Hence s is a universal function of q, H_x and H_y, and the required relationship may be evaluated when the family of profiles is specified.

At present the only system of approximate profiles with suction is that due to Schlichting.[2] This system of profiles is used here to evaluate the relationship between s and q for given H_x and H_y.

3.3. *The calculation of* s *and* q *in terms of* H_x *and* H_y

Thus the chordwise profile is

$$\left.\begin{aligned} \frac{u}{U} &= 1 - e^{\eta_x} + K_x\left[1 - e^{-\eta_x} - \sin\frac{\pi}{6}\eta_x\right], \quad 0 \leqslant \eta_x \leqslant 3 \\ &= 1 - (1 + K_x)\, e^{-\eta_x}, \qquad \eta_x \geqslant 3, \end{aligned}\right\} \tag{22}$$

where

$$\eta_x = \frac{z}{\delta_x},$$

δ_x being a measure of the chordwise boundary layer thickness.

The momentum thickness of the chordwise layer is given in its non-dimensional form by

$$\frac{\theta_x}{\delta_x} = 0{\cdot}5 + 0{\cdot}06656\,K_x - 0{\cdot}02358\,K_x^2 = g_x. \tag{23}$$

The displacement thickness is given in the same way by

$$\frac{\delta_x^*}{\delta_x} = -1 - 0{\cdot}09014\,K_x = f_x. \tag{24}$$

The form parameter H_x is therefore

$$H_x = \frac{\delta_x^*}{\theta_x} = \frac{1 - 0{\cdot}09014\,K_x}{0{\cdot}5 + 0{\cdot}06656\,K_x - 0{\cdot}02358\,K_x^2}. \tag{25}$$

The spanwise velocity profile is given by

$$\left.\begin{aligned} \frac{v}{V_0} &= 1 - e^{-\eta_y} + K_y\left[1 - e^{-\eta_y} - \sin\frac{\pi}{6}\eta_y\right], \quad 0 \leqslant \eta_y \leqslant 3 \\ &= 1 - (1 + K_y)\,e^{-\eta_y}, \qquad \eta_y \geqslant 3, \end{aligned}\right\} \tag{26}$$

where

$$\eta_y = \frac{z}{\delta_y},$$

δ_y being a measure of the spanwise boundary layer thickness.

The momentum thickness of the spanwise layer in its non-dimensional form is given by

$$\left.\begin{aligned} \frac{\theta_y}{\delta_y} &= 0{\cdot}5 + 0{\cdot}06656\,K_y - 0{\cdot}02358\,K_y^2, \\ &= g_y. \end{aligned}\right\} \tag{27}$$

Similarly, the displacement thickness is obtained in its non-dimensional form as

$$\frac{\delta_y^*}{\delta_y} = 1 - 0{\cdot}09014\,K_y = f_y. \tag{28}$$

Thus the form parameter H_y for the spanwise profile is

$$H_y = \frac{\delta_y^*}{\theta_y} = \frac{1 - 0.09014\,K_y}{0{\cdot}5 + 0{\cdot}06656\,K_y - 0{\cdot}02358\,K_y^2}. \tag{29}$$

Mixed momentum thickness.—Define

$$\gamma = \frac{\delta_y}{\delta_x},$$

and then, the mixed momentum thickness is separately calculated for the two cases, $\gamma \leqslant 1$ and $\gamma \geqslant 1$.

For $\gamma \leqslant 1$ (*i.e.*, $\delta_y > \delta_x$) the mixed momentum thickness is given by (Calculation not given here)

$$\left.\begin{aligned} \frac{\theta_{xy}}{\delta_y} &= a_0 + a_1 K_x + a_2 K_y + a_3 K_x K_y, \\ &= g_{xy} \end{aligned}\right\}. \tag{30}$$

where the coefficients a_0, a_1, a_2 and a_3 are given by

$$a_0 = 1 - \frac{1}{1+\gamma},$$

$$a_1 = 1 - \frac{1}{1+\gamma} - e^{-3/\gamma} + \frac{e^{-3/\gamma} - \frac{\pi\gamma}{6}}{1 + \left(\frac{\pi\gamma}{6}\right)^2},$$

$$a_2 = -2 + \frac{6}{\pi} + \frac{1}{\gamma} - \frac{1}{1+\gamma} - \frac{e^{-3\gamma}}{\gamma} + \frac{\gamma e^{-3\gamma} - \frac{\pi}{6}}{\gamma^2 + \left(\frac{\pi}{6}\right)^2},$$

and

$$a_3 = -2 + \frac{1}{\gamma} + \frac{6}{\pi} - \frac{1}{1+\gamma} + \frac{6}{\pi\gamma} - \frac{1}{\gamma} e^{-3\gamma} - e^{-3/\gamma}$$

$$+ \frac{\gamma e^{-3\gamma} - \frac{\pi}{6}}{\gamma^2 + \left(\frac{\pi}{6}\right)^2} + \frac{e^{-3/\gamma} - \frac{\pi\gamma}{6}}{1 + \left(\frac{\pi\gamma}{6}\right)^2} - \frac{6}{\pi}\left(\frac{1}{\gamma} + \frac{\gamma}{1-\gamma^2}\right)\cos\frac{\pi\gamma}{2}.$$

For $\gamma \geqslant 1$ (*i.e.*, $\delta_y \geqslant \delta_x$) the mixed momentum thickness is given by

$$\theta_{xy} = b_0 + b_1 K_x + b_2 K_y + b_3 K_x K_y = g_{xy} \tag{31}$$

where the coefficients b_0, b_1, b_2 and b_3 are analytically expressed as

$$b_0 = 1 - \frac{1}{1+\gamma}, \quad b_1 = 1 - \frac{1}{1+\gamma} - e^{-3/\gamma} + \frac{e^{-3/\gamma} - \frac{\pi\gamma}{6}}{1 + \left(\frac{\pi\gamma}{6}\right)^2},$$

$$b_2 = -2 + \frac{6}{\pi} + \frac{1}{\gamma} - \frac{1}{1+\gamma} - \frac{1}{\gamma} e^{-3\gamma} + \frac{\gamma e^{-3\gamma} - \frac{\pi}{6}}{\gamma^2 + \left(\frac{\pi}{6}\right)^2},$$

and

$$b_3 = 1 + \frac{6}{\pi} + \frac{1}{\gamma}\left(\frac{6}{\pi} - 2\right) - \frac{1}{1+\gamma} - e^{-3/\gamma} + \frac{e^{-3/\gamma} - \left(\frac{\pi\gamma}{6}\right)}{1 + \left(\frac{\pi\gamma}{6}\right)^2}$$

$$- \frac{1}{\gamma} e^{-3\gamma} + \frac{\gamma e^{-3\gamma} - \frac{\pi}{6}}{\gamma^2 + \left(\frac{\pi}{6}\right)^2} - \frac{6\gamma^2}{\pi(\gamma^2 - 1)} \cos \frac{\pi}{2\gamma}.$$

It is also seen that for $\gamma = 1$ the two equations (30) and (31) become identical. From equations (23), (27), (30) and (31) we get

$$\left.\begin{aligned} s &= \frac{g_{xy}}{g_x}\gamma \\ \text{and} \\ q &= \frac{g_y}{g_x}\gamma \end{aligned}\right\}. \qquad (32)$$

If K_x, K_y and γ are given, g_x, g_y and g_{xy}, and consequently s and q can be calculated.

Range of calculation.—The functions K_x and K_y determine H_x and H_y as given in equations (25) and (29) respectively. But for the present calculations H_x and H_y are supposed to be given and consequently K_x and K_y are determined. For this purpose equations (25) and (29) are identical in form and may be expressed as equation

$$0{\cdot}02358\, H_t K_t^2 - K_t\,[0{\cdot}09014 + 0{\cdot}06656\, H_t) + 1 - \tfrac{1}{2} H_t = 0 \qquad (33)$$

where K_t is a variable representing K_x or K_y. It is known from the results obtained by the present author[4] that the smallest value of H_y is 2·0 for the asymptotic suction case. This value will also be taken as the lower limit of H_x, although Thwaites[5] has obtained some values of H_x less than 2. If H_t equals the minimum value 2·0, the product of the two roots of K_t in (33) becomes zero. One root $K_t = 0$, gives the asymptotic suction profile and the other root is positive which is excluded by Schliching.[2] For all $H_t \geqslant 2$ the product of the two roots of K_t is always negative, and only the negative roots are permissible. Thus one value of H_t yields only one relevant value of K_t.

The range of H_y is given by $2 \leqslant H_y \leqslant 2{\cdot}59$ where the lower limit is fixed by the asymptotic suction profile, and the upper limit by the Blasius

profile for the flat plate. It is noted here that for any solid boundary $H_y = 2{\cdot}59$. The range of H_x is taken to be $2 \leqslant H_x = 4$. The choice of the upper limit is a bit arbitrary, but it is expected that calculations of the boundary layer will not be normally taken beyond $H_x = 4$. This limit can be extended beyond 4·0 if necessary but it is not proposed to do so here.

Results of the calculations.—For given values of H_x and H_y, K_x and K_y are obtained by equation (33). These values of K_x, K_y together with suitable values of γ determine s and q with equation (32). Curves of s and q for two extreme cases $H_x = 2{\cdot}0$ and $H_x = 4{\cdot}0$ for $H_y = 2{\cdot}0$, 2·1, 2·2, 2·3, 2·4, 2·5 and 2·6 are shown in Figures 3 and 4. For given H_x, H_y and s, q can be obtained from tables or curves obtained for s and q for given H_x and H_y.

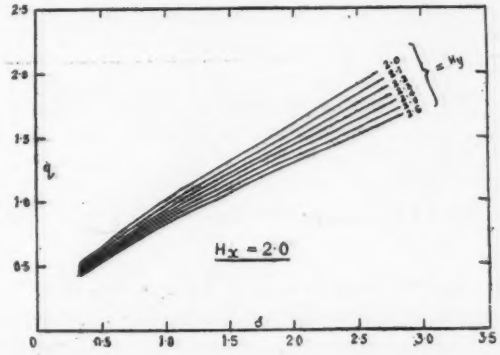

FIG. 3. Curves for calculating q for $H_x = 2{\cdot}0$ and arbitrary values of H_y and s.

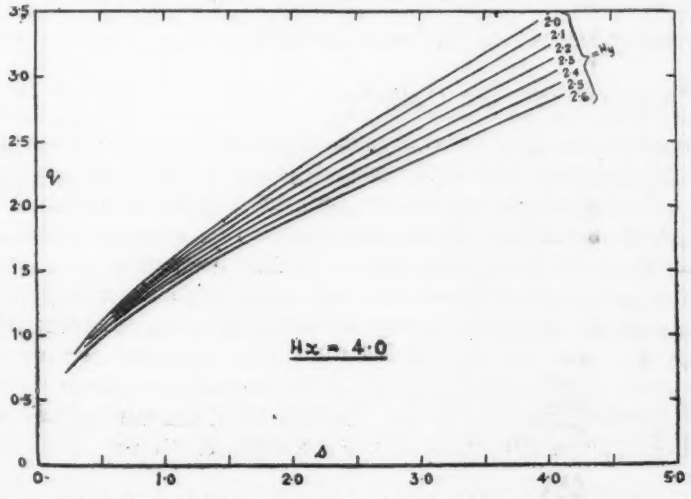

FIG. 4. Curves for calculating q for $H_x = 4{\cdot}0$ and arbitrary values of H_y and s.

3.4. *Method for the calculation of H_y*

It has been mentioned in Section 3.1 that λ_y depends only on suction and may be taken as a suction-parameter. Thus H_y depending on suction only may be taken as a function of λ_y only. The relationship between H_y and λ_y is now required in the application of the method as obtained in Section 3.0. This relationship can be evaluated using Schlichting's[2] approximate profiles as was done for s and q in Section 3.3. But it is expected to obtain better results by the use of the well-known exact solution given by Iglisch[3] for the flat plate with uniform suction.

Iglisch[3] gives a table of λ_y and H_y, and for convenience, the values are reproduced here in Fig. 5.

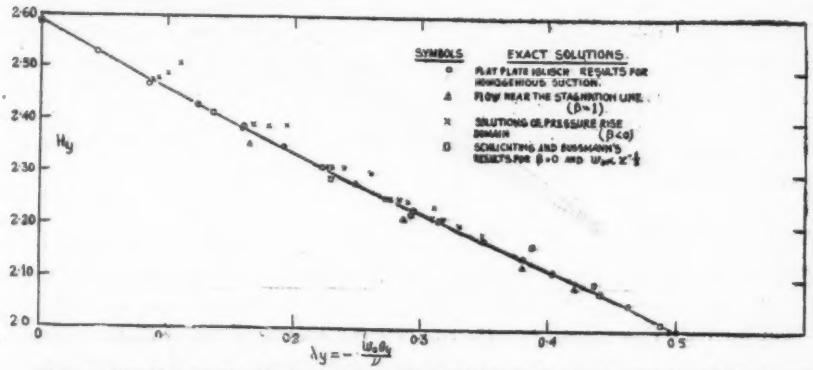

FIG. 5. Variation of the shape-parameter H_y with the suction parameter λ_y of the spanwise boundary layer based on some exact solutions.

3.5. *Comparison with exact solutions*

Comparison of q *with exact solutions.*—In Section 3.3 the universal relationship between s and q for given H_x and H_y has been evaluated by the use of Schlichting's[2] system of approximate velocity profiles. Before applying these results to any general calculation on a yawed cylinder, it is desirable to estimate their accuracy. For this comparison it is assumed here that H_x, H_y and s are given correctly and only the values of q are compared from the two sources. The typical cases of flow chosen for this purpose are:—the flat plate with zero pressure gradient, the flow near chordwise stagnation line with constant suction, and some suitable cases of flow with adverse pressure gradients and suction for the chordwise velocity distribution $U = Cx^m (m < 0)$ at the edge of the boundary layer.

It is known that on a flat plate either with or without suction, the solutions of the two boundary layers (chordwise and spanwise) are identical. Hence $H_x = H_y$, $s = 1$ and $q = 1$. From Fig. 3 it is seen that for $H_x = H_y$ and $s = 1$, q is always one.

For the flow near the chordwise stagnation line with constant suction ($U = Cx$), the comparison is made with the exact solutions and the results show that the percentage error is less than 0·5.

For cases of flow with adverse pressure gradients and suction ($U = Cx^m$, $m \angle 0$), results of the comparison show that the errors in the calculations are less than 6 per cent. even when large suctions are applied.

Comparison of H_y with exact solutions.—In this comparison λ_y is supposed given and values of H_y from exact solutions are compared with the values of H_y obtained from Iglisch.[3] The same typical cases are compared here also. These exact values of H_y are plotted against λ_y in Fig. 5 and are seen to lie approximately on the Iglisch[3] curve.

The percentage of error involved is also less than 3 even for adverse pressure gradients.

3.6. *Procedure for practical calculation*

To carry out the calculation of the spanwise layer, the results of the chordwise layer are assumed to be given. The calculation may start from any point, where the characteristics of the spanwise layer are known. Generally, it starts from the stagnation point where q and s can be determined. If the suction does not start at the stagnation point, H_y is known to be 2·59 and H_x will be already given from the chordwise layer.

Hence, q and s can be simultaneously obtained by the intersection of the curve of s against q for given H_x and H_y (from the universal relationship) with the curve $sq = 3$ [deduced from equation (17) at the stagnation point]. If the suction starts from the leading edge, the procedure is slightly different. In this case use is made of the exact solution at the stagnation point with constant suction. If one uses the exact values of q, s and H_y directly as the initial conditions, results are bound to fluctuate for one or two steps. This happens so, firstly because the simplified momentum equation (16) is not satisfied exactly, and secondly because the characteristics of the spanwise layer at this point are not strictly related to the given chordwise results (by an approximate method). Therefore, first of all H_y is fixed from the exact solution for given λ_x which is known from the chordwise

flow. Then for given H_x and H_y, $q-s$ curve is drawn according to Section 3.3. Another curve relating q and s is obtained from (16) near stagnation as

$$qs = \frac{0{\cdot}225 - 0{\cdot}64\, q\lambda_x + 0{\cdot}38\, q^2\lambda_x^2}{\frac{U'\theta_x^2}{\nu}}, \tag{34}$$

where

$$\lambda_x \quad \text{and} \quad \frac{U'\theta_x^2}{\nu}$$

are given from the chordwise flow. The first set of values of q and s is obtained by the intersection of the above two curves. Then $\lambda_y = q\lambda_x$ is determined and hence a second value of H_y is obtained from the given Iglisch curve. If there is no difference between the two values of H_y, the initial conditions are satisfactory. If there is any difference, the calculation cycle is repeated. In this way values of s, q, λ_y and H_y at the starting point are determined.

The calculation then proceeds as follows: The gradient

$$\left[\frac{d}{dx}(sU\theta_x)\right]_{x=x_0}$$

at the starting point is calculated by equation (16). The quantity $sU\theta_x$ at the next point x_1 is obtained from the relation,

$$(sU\theta_x)_{x=x_1} = (sU\theta_x)_{x=x_0} + (x_1 - x_0)\left[\frac{d}{dx}(sU\theta_x)\right]_{x=x_0}. \tag{35}$$

Thus s is known at the point x_1, since U and θ_x are given. To determine q at x_1, H_y is tentatively taken to be the same as at x_0. This procedure is supported by the fact that H_y is constant near stagnation (exact solution). q is then obtained from the results of Section 3.3 for known H_x, H_y and s. λ_y is calculated by the relation $\lambda_y = q\lambda_x$ which again determines H_y from the Iglisch[3] table or curve. If there is any difference between the two values of H_y, the cycle of calculation is repeated, and if not, the calculation proceeds to the next step.

When more than two values of H_y become known, tentative value of H_y may be chosen from graphical extrapolation. For a solid boundary H_y is constant ($H_y = 2{\cdot}59$) and no extrapolation is necessary.

It has been found in practice that one cycle of calculation is usually enough, and in no case were more than two cycles required.

3.7. *Discussion and conclusion*

The present approximate method for calculating the laminar spanwise layer on an infinite uniform yawed cylinder is mainly constructed for a porous boundary, but it may also be applicable for a solid boundary. The method has given very good agreement with the exact solutions of the spanwise layer for the chordwise velocity distribution $U = Cx^m$ at the edge of the layer. The results of the chordwise layer are assumed to be known. This assumption of exact knowledge of the chordwise layer is an ideal which will not be realised in practice. Any error involved in the approximate calculation of the chordwise layer will be automatically inherited in the calculation of the spanwise layer. In addition to this unknown source of error, the method may be expected to be fairly inaccurate after Schlichting's[2] separation at

$$\frac{U'\theta_x^2}{\nu} = -\ 0{\cdot}0682.$$

This inaccuracy is the intrinsic weakness of Schlichting's[2] profiles for which there appears no remedy at the moment. However, no approximate method at present gives very satisfactory results in regions of increasing pressure. But it should be noted that the calculation may be continued even after this so-called separation point, if necessary.

4. References

1. Rott, N. and Crabtree, L. F. .. "Simplified laminar boundary layer calculation for bodies of revolution and for yawed wings," *Journal of the Aeronautical Sciences*, August 1952, **19** (8).

2. Schlichting, H. .. "An approximate method for the calculation of the laminar boundary layer with suction for bodies of arbitrary shape," *N.A.C.A.T.M.*, 1216, 1949.

3. Iglisch, R. .. "Exact calculation of laminar boundary layer in longitudinal flow over a flat plate with homogeneous suction," *Ibid.*, 1205, 1949.

4. Sinha, K. D. P. .. "The laminar boundary layer on an infinite uniform yawed cylinder with distributed suction for the chordwise potential velocity distribution $U = Cx^m$, C.P. No. 214, *A.R.C.T.R.* 17183, 11th November, 1954.

5. Thwaites, B. .. "The development of the laminar boundary layer under conditions of continuous suctions. Part II. Approximate methods of solutions," *A.R.C.*, 12699, F.M. 1296 *a*, 1949.

6. Lin, C. C. .. *The Theory of Hydrodynamic Stability*, Cambridge University Press, 1955.

FLOW OF NON-NEWTONIAN FLUID BETWEEN TORSIONALLY OSCILLATING DISCS

By (Miss) G. K. Rajeswari

(*Department of Applied Mathematics, Indian Institute of Science, Bangalore-12*)

Received May 30, 1961

(Communicated by Prof. P. L. Bhatnagar, F.A.SC.)

1. Introduction

A theoretical analysis is made of the flow of an incompressible non-Newtonian viscous fluid contained between two torsionally oscillating infinite parallel discs on lines similar to those of the corresponding Newtonian case considered by Rosenblat. We study the two cases where (i) one disc only is oscillating torsionally while the other is at rest and (ii) both the discs oscillate with the same frequency and amplitude but the motions at any instant are in opposite directions. Assuming that the amplitude of the oscillation namely (Ω/n) is small and neglecting the terms of $0(\Omega/n)^2$ in the equations of motion in comparison with terms of $0(\Omega/n)$ we solve exactly for the velocity field and pressure satisfying all the boundary conditions completely. This approximation gives the same transverse velocity field as in the Newtonian case obtained by Rosenblat. We find that the radial-axial flow has a mean steady component and a fluctuating component of frequency twice that of the oscillating disc. We observe that the approximations made gives the velocity field valid only for small Reynolds numbers unlike the Newtonian case, where the asymptotic expansion of the velocity field for large Reynolds numbers has also been obtained. We have studied the non-Newtonian effects on the streamlines of the steady part of the radial-axial flow and on the steady component of the radial velocity in both the cases through a dimensionless parameter $S = (\nu_c/d^2)$, where ν_c is the kinematic coefficient of cross-viscosity assumed as constant and d is the distance between the plates. We have compared the flow of the Newtonian case ($S = 0$) with the non-Newtonian case considering both negative and positive values of S. We observe the continuity of the effect as S changes from negative to positive values. We have derived the expressions for the shearing stresses acting on the plates for small Reynolds numbers.

1. We consider a body of non-Newtonian fluid bounded by two infinite parallel plane discs which are represented by the planes $z = 0$ and $z = d$

in a cylindrical polar co-ordinate system. The discs perform torsional oscillations about the axis, $r = 0$. If w, v, w are respectively the radial, transverse and axial velocity components, p, the pressure, ρ, the density, μ, μ_c, the coefficients of viscosity and cross-viscosity and ν, ν_c, the kinematic coefficients of viscosity, the equations of motion of a non-Newtonian fluid in cylindrical polar co-ordinate system are:

$$\begin{aligned}
&\frac{\partial u}{\partial t} + u\frac{\partial u}{\partial r} + w\frac{\partial u}{\partial z} - \frac{v^2}{r} \\
&\quad = -\frac{1}{\rho}\frac{\partial p}{\partial r} + \nu\left\{\frac{\partial^2 u}{\partial r^2} + \frac{\partial^2 u}{\partial z^2} + \frac{1}{r}\frac{\partial u}{\partial r} - \frac{u}{r^2}\right\} \\
&\qquad + 2\nu_c\left\{4\frac{\partial u}{\partial r}\frac{\partial^2 u}{\partial r^2} + \left(\frac{\partial u}{\partial z} + \frac{\partial w}{\partial r}\right)\left(\frac{\partial^2 u}{\partial r \partial z} + \frac{\partial^2 w}{\partial r^2}\right)\right. \\
&\qquad - \frac{u}{r}\frac{\partial^2 w}{\partial r \partial z} - \frac{u}{r}\frac{\partial^2 u}{\partial z^2} - \frac{1}{2r}\left(\frac{\partial u}{\partial z}\right)^2 + \frac{1}{2r}\left(\frac{\partial w}{\partial r}\right)^2 \\
&\qquad \left. + \frac{2}{r}\left(\frac{\partial u}{\partial r}\right)^2 - \frac{2u^2}{r^3}\right\} + \nu_c\left\{2\left(\frac{\partial v}{\partial r} - \frac{v}{r}\right)\frac{\partial}{\partial r}\left(\frac{\partial v}{\partial r} - \frac{v}{r}\right)\right. \\
&\qquad \left. + \frac{\partial v}{\partial z}\frac{\partial}{\partial z}\left(\frac{\partial v}{\partial r} - \frac{v}{r}\right) - \frac{1}{r}\left(\frac{\partial v}{\partial z}\right)^2 + \left(\frac{\partial v}{\partial r} - \frac{v}{r}\right)\frac{\partial^2 v}{\partial z^2}\right\}, \qquad (1.1)
\end{aligned}$$

$$\begin{aligned}
&\frac{\partial v}{\partial t} + u\frac{\partial v}{\partial r} + w\frac{\partial v}{\partial z} + \frac{uv}{r} \\
&\quad = \nu\left\{\frac{\partial^2 v}{\partial r^2} + \frac{\partial^2 v}{\partial z^2} + \frac{1}{r}\frac{\partial v}{\partial r} - \frac{v}{r^2}\right\} + \nu_c\left\{\frac{\partial^2 v}{\partial r \partial z}\left(\frac{\partial u}{\partial z} + \frac{\partial w}{\partial r}\right)\right. \\
&\qquad + \frac{\partial v}{\partial z}\frac{\partial}{\partial r}\left(\frac{\partial u}{\partial z} + \frac{\partial w}{\partial r}\right) - 2\frac{\partial^2 u}{\partial r \partial z}\frac{\partial v}{\partial z} + \left(\frac{\partial u}{\partial z} + \frac{\partial w}{\partial r}\right)\frac{\partial}{\partial z} \\
&\qquad \times\left(\frac{\partial v}{\partial r} - \frac{v}{r}\right) + \left(\frac{\partial v}{\partial r} - \frac{v}{r}\right)\frac{\partial}{\partial z}\left(\frac{\partial u}{\partial z} + \frac{\partial w}{\partial r}\right) \\
&\qquad - 2\frac{\partial w}{\partial z}\frac{\partial}{\partial r}\left(\frac{\partial v}{\partial r} - \frac{v}{r}\right) - 2\frac{\partial^2 v}{\partial z^2}\frac{\partial u}{\partial r} - 2\frac{\partial^2 w}{\partial r \partial z}\left(\frac{\partial v}{\partial r} - \frac{v}{r}\right) \\
&\qquad \left. - \frac{4}{r}\frac{\partial w}{\partial z}\left(\frac{\partial v}{\partial r} - \frac{v}{r}\right) + \frac{2}{r}\left(\frac{\partial u}{\partial z} + \frac{\partial w}{\partial r}\right)\frac{\partial v}{\partial z}\right\}, \qquad (1.2)
\end{aligned}$$

$$\frac{\partial w}{\partial t} + u\frac{\partial w}{\partial r} + w\frac{\partial w}{\partial z}$$

$$= -\frac{1}{\rho}\frac{\partial p}{\partial z} + \nu\left\{\frac{\partial^2 w}{\partial r^2} + \frac{\partial^2 w}{\partial z^2} + \frac{1}{r}\frac{\partial w}{\partial r}\right\}$$

$$+ 2\nu_c\left\{4\frac{\partial w}{\partial z}\frac{\partial^2 w}{\partial z^2} - \frac{u}{r}\frac{\partial^2 u}{\partial r\partial z} - \frac{u}{r}\frac{\partial^2 w}{\partial r^2} - \frac{1}{r}\frac{\partial u}{\partial r}\frac{\partial u}{\partial z}\right.$$

$$\left. - \frac{1}{r}\frac{\partial u}{\partial r}\frac{\partial w}{\partial r} + \left(\frac{\partial u}{\partial z} + \frac{\partial w}{\partial r}\right)\left(\frac{\partial^2 u}{\partial z^2} + \frac{\partial^2 w}{\partial r\partial z}\right)\right\}$$

$$+ \nu_c\left\{\frac{\partial v}{\partial z}\left(2\frac{\partial^2 v}{\partial z^2} + \frac{\partial^2 v}{\partial r^2}\right) + \frac{\partial^2 v}{\partial r\partial z}\left(\frac{\partial v}{\partial r} - \frac{v}{r}\right)\right\}, \tag{1.3}$$

and

$$\frac{\partial u}{\partial r} + \frac{u}{r} + \frac{\partial w}{\partial z} = 0. \tag{1.4}$$

2. One Disc Oscillating

We consider the disc at $z = 0$ to perform torsional oscillations of frequency n and angular speed Ω, while the disc at $z = d$, remains at rest.

Following Rosenblat, we assume the velocity field as

$$\left.\begin{aligned} u &= r\frac{\Omega^2}{n}\frac{\partial}{\partial y}\mathrm{F}(y, \tau), \\ v &= r\Omega e^{i\tau} g(y), \\ w &= -2d\frac{\Omega^2}{n}\mathrm{F}(y, \tau), \end{aligned}\right\} \tag{2.1}$$

where

$$y = \frac{z}{d} \quad \text{and} \quad \tau = nt.$$

Further we assume that

$$\frac{p}{\rho} = \frac{\Omega^2 r^2}{2}\mathrm{P}(y, \tau) + 2\Omega^2 d^2 \mathrm{K}(y, \tau). \tag{2.2}$$

The equation of continuity (1.4) is identically satisfied by such a choice of velocity field. The boundary conditions of the problem are

$$u = w = 0, \qquad v = \mathrm{Re}(r\Omega e^{int}) \qquad \text{at } z = 0, \tag{2.3}$$

and

$$u = v = w = 0 \qquad \text{at} \qquad z = d. \tag{2.4}$$

Substituting (2.1) and (2.2) in the equations of motion (1.1) to (1.3) we have

$$\frac{\partial^2 F}{\partial y \partial \tau} + \left(\frac{\Omega}{n}\right)^2 \left[\left(\frac{\partial F}{\partial y}\right)^2 - 2F\frac{\partial^2 F}{\partial y^2}\right] - [e^{i\tau} g(y)]^2$$

$$= -P(y, \tau) + \frac{1}{R}\frac{\partial^3 F}{\partial y^3} + S\left(\frac{\Omega}{n}\right)^2 \left[\left(\frac{\partial^2 F}{\partial y^2}\right)^2 - \frac{\partial F}{\partial y}\frac{\partial^3 F}{\partial y^3}\right]$$

$$- S\left[e^{i\tau}\frac{dg}{dy}\right]^2, \tag{2.5}$$

$$ig(y) + 2\left(\frac{\Omega}{n}\right)^2 \left[g\frac{\partial F}{\partial y} - F\frac{dg}{dy}\right]$$

$$= \frac{1}{R}\frac{d^2 g}{dy^2} + 2\left(\frac{\Omega}{n}\right)^2 S\left[\frac{dg}{dy}\frac{\partial^2 F}{\partial y^2} - \frac{\partial F}{\partial y}\frac{\partial^2 g}{dy^2}\right], \tag{2.6}$$

and

$$2\frac{\partial F}{\partial \tau} - 4\left(\frac{\Omega}{n}\right)^2 F\frac{\partial F}{\partial y}$$

$$= \frac{r^2}{d^2}\left[\frac{1}{2}\frac{\partial P}{\partial y} - 2Se^{2i\tau}\frac{dg}{dy}\frac{d^2 g}{dy^2} - 2S\left(\frac{\Omega}{n}\right)^2 \frac{\partial^2 F}{\partial y^2}\frac{\partial^3 F}{\partial y^3}\right]$$

$$+ \frac{2}{R}\frac{\partial^2 F}{\partial y^2} + 2\frac{\partial K}{\partial y} - 28S\left(\frac{\Omega}{n}\right)^2 \frac{\partial F}{\partial y}\frac{\partial^2 F}{\partial y^2}, \tag{2.7}$$

where

$$S = \frac{\nu_e}{d^2} \qquad \text{and} \qquad R = \frac{nd^2}{\nu}.$$

The boundary conditions transform to

$$F = \frac{\partial F}{\partial y} = 0, \qquad g = 1 \qquad \text{at } y = 0, \tag{2.8}$$

and

$$F = \frac{\partial F}{\partial y} = g = 0 \qquad \text{at } y = 1. \tag{2.9}$$

On the assumption that the amplitude of the oscillations namely Ω/n is small, retaining only the first order terms in Ω/n, we have for the transverse velocity component

$$\left.\begin{aligned} & ig(y) = \frac{1}{\mathrm{R}} \frac{d^2g}{dy^2} \\ \text{with} \\ & g(0) = 1 \quad \text{and} \quad g(1) = 0. \end{aligned}\right\} \tag{2.10}$$

The solution of (2.10) is

$$g(y) = \frac{\sinh \sqrt{i\mathrm{R}}\,(1-y)}{\sinh \sqrt{i\mathrm{R}}}, \tag{2.11}$$

same as obtained by Rosenblat in the Newtonian case.

For small Reynolds numbers we have

$$\frac{v}{r\Omega} = (1-y)\left\{\left[1 - \frac{\mathrm{R}^2}{360}\, y\,(8 + 8y - 12y^2 + 3y^3)\right]\cos nt + \frac{\mathrm{R}}{6}\, y\,(2-y)\sin nt\right\} + 0(\mathrm{R}^3).$$

Neglecting the terms of order $(\Omega/n)^2$, we have from (2.5) for the radial-axial component of velocity

$$\frac{\partial^2 \mathrm{F}}{\partial y\,\partial \tau} - [ge^{i\tau}]^2 = -\mathrm{P}(y,\tau) + \frac{1}{\mathrm{R}} \frac{\partial^3 \mathrm{F}}{\partial y^3} - \mathrm{S}\left[e^{i\tau} \frac{dg}{dy}\right]^2. \tag{2.12}$$

From (2.7) we have

$$\frac{\partial \mathrm{F}}{\partial \tau} = \frac{1}{\mathrm{R}} \frac{\partial^2 \mathrm{F}}{\partial y^2} + \frac{\partial \mathrm{K}}{\partial y}, \tag{2.13}$$

and equating the coefficient of r^2 to zero we have

$$\frac{1}{2} \frac{\partial \mathrm{P}}{\partial y} - 2\mathrm{S}e^{2i\tau} \frac{dg}{dy} \frac{d^2g}{dy^2} = 0, \tag{2.14}$$

which determines $\mathrm{P}(y, \tau)$.

Let

$$\mathrm{F}(y, \tau) = f(y) + h(y)\, e^{2i\tau}, \tag{2.15}$$

and

$$K(y, \tau) = K_0(y) + K_1(y)\, e^{2i\tau}. \tag{2.16}$$

From (2.14) we have

$$\frac{P}{2} - Se^{2i\tau}\left(\frac{dg}{dy}\right)^2 = a(\tau). \tag{2.17}$$

Substituting (2.15), (2.16) and (2.17) in (2.12) and (2.13) we have

$$2ih'(y)\, e^{2i\tau} - [ge^{i\tau}]^2$$

$$= -2a(\tau) - 3S\left[e^{i\tau}\frac{dg}{dy}\right]^2 + \frac{1}{R}[f'''(y) + h'''(y)\, e^{2i\tau}], \tag{2.18}$$

and

$$2ih(y)\, e^{2i\tau} = \frac{1}{R}[f'''(y) + h'''(y)\, e^{2i\tau}] + \frac{d}{dy}K_0(y)$$

$$+ \frac{d}{dy}K_1(y)\, e^{2i\tau}. \tag{2.19}$$

These equations are sufficient to determine the unknowns $f(y)$, $h(y)$, $K_0(y)$ and $K_1(y)$. The above equations indicate that the radial-axial flow has a mean steady component and a fluctuating component of frequency twice that of the oscillating plate. From (2.11) we have

$$[g(y)]^2 e^{2i\tau} = \frac{1}{2}\left[\frac{\cosh \lambda y_1 - \cos \lambda y_1}{\cosh \lambda - \cos \lambda}\right] + \frac{1}{2}\left[\frac{\cosh \lambda(1+i)\, y_1 - 1}{\cosh \lambda(1+i) - 1}\right] e^{2i\tau}, \tag{2.20}$$

and

$$\left[\frac{dg}{dy}\right]^2 e^{2i\tau} = \frac{\lambda^2}{4}\left[\frac{\cosh \lambda y_1 + \cos \lambda y_1}{\cosh \lambda - \cos \lambda}\right]$$

$$+ \frac{i\lambda^2}{4}\left[\frac{\cosh \lambda(1+i)\, y_1 + 1}{\cosh \lambda(1+i) - 1}\right] e^{2i\tau}, \tag{2.21}$$

where

$$\lambda = \sqrt{2R} \quad \text{and} \quad y_1 = 1 - y.$$

Substitution of (2.20) and (2.21) into (2.18) yields

$$\frac{f'''(y)}{R} = L_0 + 3S\frac{\lambda^2}{4}\left[\frac{\cosh \lambda y_1 + \cos \lambda y_1}{\cosh \lambda - \cos \lambda}\right] - \frac{1}{2}\left[\frac{\cosh \lambda y_1 - \cos \lambda y_1}{\cosh \lambda - \cos \lambda}\right], \tag{2.22}$$

and

$$\frac{1}{R}h'''(y) - 2ih'(y)$$

$$= L_1 + 3S\frac{\lambda^2}{4}\left[\frac{\cosh \lambda(1+i)y_1 + 1}{\cosh \lambda(1+i) - 1}\right]$$

$$- \frac{1}{2}\left[\frac{\cosh \lambda(1+i)y_1 - 1}{\cosh \lambda(1+i) - 1}\right], \tag{2.23}$$

where we have taken

$$2a(\tau) = L_0 + L_1 e^{2i\tau}.$$

The boundary conditions (2.8), (2.9) reduce to

$$f = f' = 0 \quad \text{at } y = 0 \quad \text{and} \quad y = 1, \tag{2.24}$$

and

$$h = h' = 0 \quad \text{at } y = 0 \quad \text{and} \quad y = 1. \tag{2.25}$$

The solution of (2.22) for the mean steady component under the conditions (2.24) is found to be

$$f(y) = \left[\frac{1}{\cosh \lambda - \cos \lambda}\right]\left\{\left[\frac{1}{4\lambda}(\sinh \lambda y_1 + \sin \lambda y_1)\right.\right.$$

$$+ \frac{1}{4}y(1-y)^2(\cosh \lambda + \cos \lambda) - \frac{1}{4\lambda}(1 - 3y^2 + 2y^3)$$

$$\times (\sinh \lambda + \sin \lambda) - \left.\frac{1}{2}y^2(1-y)\right] + 3S\frac{\lambda}{8}$$

$$\left.\times [(2y^3 - 3y^2 + 1)(\sinh \lambda - \sin \lambda) - (\sinh \lambda y_1 - \sin \lambda y_1)]\right\}$$

$$- 3S\frac{\lambda^2}{8}y(1-y)^2, \tag{2.26}$$

and

$$f'(y) = \left[\frac{1}{\cosh\lambda - \cos\lambda}\right]\left\{\left[-\frac{1}{4}(\cosh\lambda y_1 + \cos\lambda y_1)\right.\right.$$
$$+ \frac{3}{2\lambda} y(1-y)(\sinh\lambda + \sin\lambda) + \frac{1}{4}(1 - 4y + 3y^2)$$
$$\times (\cosh\lambda + \cos\lambda) - \frac{1}{2} y(2 - 3y)\Big]$$
$$+ 3S\frac{\lambda^2}{8}\left[\cosh\lambda y_1 - \cos\lambda y_1) + \frac{6}{\lambda} y(y-1)\right.$$
$$\left.\left.\times (\sinh\lambda - \sin\lambda)\right]\right\} + 3S\frac{\lambda^2}{8}(4y - 1 - 3y^2). \qquad (2.27)$$

For small Reynolds numbers we have

$$f(y) \approx \frac{R}{120} y^2(1-y)^2\left\{(3-y) + \frac{R^2}{3780}[-5y^5 + 35y^4\right.$$
$$- 105y^3 + 175y^2 - 133y - 21]$$
$$\left.+ \frac{R^2 S}{7}[y^3 - 5y^2 + 10y - 10)]\right\} + 0(R^5), \qquad (2.28)$$

and

$$f'(y) \approx \frac{R}{120} y(1-y)\left\{(6 - 15y + 5y^2)\right.$$
$$- \frac{R^2}{3780}[42 - 1365y^2 + 45(-y^6 + 7y^5 - 21y^4 + 35y^3 + 7y)]$$
$$\left.- \frac{R^2 S}{7}[7(y^4 - 5y^3 + 10y^2 - 10y) + 20]\right\} + 0(R^5). \qquad (2.29)$$

The solutions for $S = 0$, corresponding to the Newtonian case are in agreement with those of Rosenblat.

The unsteady component of the radial-axial flow is given by the equation (2.23). We have

$$4[\cosh\lambda(1+i) - 1]\left[\cosh\frac{\lambda(1+i)}{\sqrt{2}} - 1 - \frac{\lambda(1+i)}{2\sqrt{2}}\right.$$
$$\left.\sinh\frac{\lambda(1+i)}{\sqrt{2}}\right] h(y)$$

$$= \left(3S\frac{\lambda^2}{4} + \frac{i}{2}\right)\left\{\left[1 - \cosh\lambda\frac{(1+i)}{\sqrt{2}}\right]\left[y\left(1 + \cosh\lambda(1+i)\right)\right.\right.$$

$$+ \frac{\sqrt{2}}{\lambda(1+i)}\sinh\frac{\lambda(1+i)}{\sqrt{2}}\,y\left(\cosh\lambda(1+i) - 1\right)$$

$$- \frac{2}{\lambda(1+i)}\sinh\lambda(1+i)\cosh\frac{\lambda(1+i)}{\sqrt{2}}\,y$$

$$\left.+ \frac{2}{\lambda(1+i)}\sinh\lambda(1+i)\,y_1\right] + \left[1 - \cosh\frac{\lambda(1+i)}{\sqrt{2}}\,y\right]$$

$$\times\left[(-1 + \cosh\lambda(1+i)\cosh\frac{\lambda(1+i)}{\sqrt{2}} - \frac{1}{\sqrt{2}}\right.$$

$$\times\sinh\lambda(1+i)\sinh\frac{\lambda(1+i)}{\sqrt{2}} + \frac{\sinh\lambda(1+i)}{\lambda(1+i)}$$

$$\times\cosh\frac{\lambda(1+i)}{\sqrt{2}} + \frac{\sqrt{2}}{\lambda(1+i)}\sinh\frac{\lambda(1+i)}{\sqrt{2}}$$

$$\left.\times\left(1 - \cosh\lambda(1+i)\right) - \frac{\sinh\lambda(1+i)}{\lambda(1+i)}\right]$$

$$+\left[\frac{1}{\sqrt{2}}\sinh\lambda(1+i)\sinh\frac{\lambda(1+i)}{\sqrt{2}}\left\{y - \frac{\sqrt{2}}{\lambda(1+i)}\right.\right.$$

$$\left.\times\sinh\frac{\lambda(1+i)}{\sqrt{2}}\,y\right\} - \frac{1}{\sqrt{2}}\sinh\frac{\lambda(1+i)}{\sqrt{2}}$$

$$\times\left\{-\sinh\lambda(1+i)\,y_1 + \sinh\lambda(1+i)\cosh\frac{\lambda(1+i)}{\sqrt{2}}\,y\right.$$

$$\left.\left.\left.- \sqrt{2}\cosh\lambda(1+i)\sinh\frac{\lambda(1+i)}{\sqrt{2}}\,y\right\}\right]\right\}. \qquad (2.30)$$

For small Reynolds numbers we get,

$$h(y) \approx \frac{\mathrm{R}}{120}y^2(1-y)^2\left\{(3-y)(1 - 3i\mathrm{RS})\right.$$

$$\left.- \frac{i\mathrm{R}}{210}(30y^3 - 150y^2 + 167y + 29)\right\} + 0(\mathrm{R}^3). \qquad (2.31)$$

The shearing stresses for the velocity field (2.1) are given by

$$T_{rz} = \frac{\partial u}{\partial z}\left[(\mu - 2\mu_c \frac{u}{r}\right],$$

$$T_{\theta z} = \frac{\partial v}{\partial z}\left[\mu - 2\mu_c \frac{\partial u}{\partial r}\right],$$

and

$$T_{r\theta} = \mu_c \frac{\partial u}{\partial z}\frac{\partial v}{\partial z}.$$

For small Reynolds numbers the shearing stresses acting on the plate $z = 0$ are given by

$$T_{rz} = \mu \frac{r}{d}\frac{\Omega^2}{n}\frac{R}{20}\left[1 + \cos 2nt + R\left(3S + \frac{29}{630}\right)\sin 2nt\right] + 0(R^3),$$

$$T_{\theta z} = -\mu \frac{r}{d}\Omega\left[\left(1 + \frac{R^2}{45}\right)\cos nt - \frac{R}{3}\sin nt\right] + 0(R^3),$$

and

$$T_{r\theta} = -\mu_c \frac{r^2}{d^2}\frac{\Omega^2}{n}\frac{R}{40}\left[\cos 3nt + 3\cos nt\right.$$

$$\left. + R\left(3S - \frac{181}{630}\right)(\sin 3nt + \sin nt)\right] + 0(R^3).$$

The shearing stresses acting on the disc $z = d$ are

$$T_{rz} = \mu \frac{r}{d}\frac{\Omega^2}{n}\frac{R}{30}\left[1 + \cos 2nt + R\left(3S + \frac{19}{105}\right)\sin 2nt\right] + 0(R^3).$$

$$T_{\theta z} = -\mu \frac{r}{d}\Omega\left[\left(1 - \frac{7R^2}{360}\right)\cos nt + \frac{R}{6}\sin nt\right] + 0(R^3),$$

and

$$T_{r\theta} = -\mu_c \frac{r^2}{d^2}\frac{\Omega^2}{n}\frac{R}{60}\left[\cos 3nt + 3\cos nt\right.$$

$$\left. + R\left(3S + \frac{73}{210}\right)(\sin 3nt + \sin nt)\right] + 0(R^3).$$

Figure 1 represents the effect of non-Newtonian term on the typical streamlines of the steady component of the flow. We have drawn the curves for $S = -0{\cdot}5$, $-0{\cdot}1$, 0 and $+0{\cdot}05$. We observe the continuity of the effect as the parameter 'S' changes from negative to positive values. The negative non-Newtonian coefficient flattens the streamline while the positive coefficient makes it more curved. Figure 2 shows the dimensionless steady

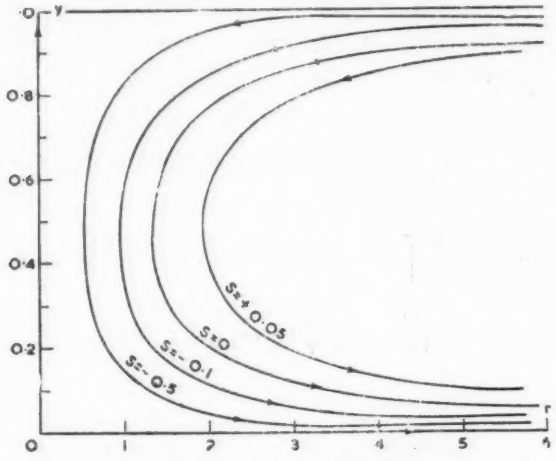

FIG. 1. One disc oscillating: Streamlines of steady radial-axial flow for $R = 5$ and $S = -0{\cdot}5$, $-0{\cdot}1$, 0, $+0{\cdot}05$.

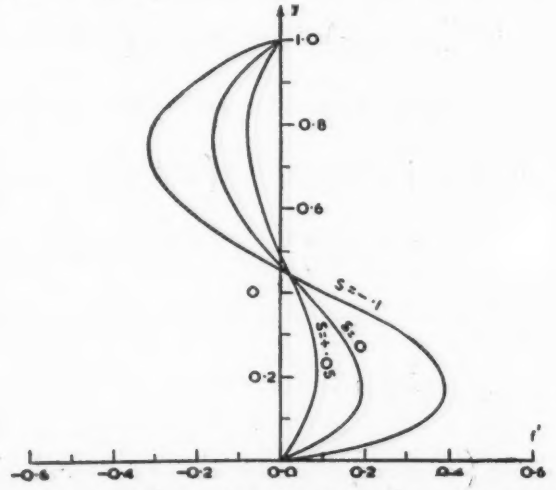

FIG. 2. One disc oscillating: Steady radial velocity f' for $S = -0{\cdot}1$, 0, $+0{\cdot}05$.

component of the radial velocity, namely, f' for S $= -0{\cdot}1$, 0 and $+0{\cdot}05$. We find $f' = 0$ at $y = 0{\cdot}45$ for S $= -0{\cdot}1$ and at $y = 0{\cdot}48$ for S $= +0{\cdot}05$.

3. Both Discs Oscillating

We now consider the case where the two discs are oscillating with same frequency and angular speed but in opposite directions. The boundary conditions in the present case are

$$\left.\begin{aligned} &u = w = 0, \quad v = \mathrm{Re}\,(r\Omega e^{int}) \qquad \text{at } z = 0, \\ &\text{and} \\ &u = w = 0, \quad v = -\mathrm{Re}\,(r\Omega e^{int}) \qquad \text{at } z = d. \end{aligned}\right\} \tag{3.1}$$

The equations of motion (1.1) to (1.3) can again be transformed by the choice of the velocity field (2.1) in a similar way and for the transverse flow we have

$$\frac{d^2g}{dy^2} - i\mathrm{R}g = 0 \tag{3.2}$$

as previously but with $g(0) = 1$, $g(1) = -1$.

The solution now is

$$g(y) = \frac{\sinh \sqrt{i\mathrm{R}}\, y_1 - \sinh \sqrt{i\mathrm{R}}\, y}{\sinh \sqrt{i\mathrm{R}}}, \tag{3.3}$$

once again the same as that obtained by Rosenblat.

For small Reynolds numbers this yields the velocity profile

$$\frac{v}{r\Omega} \approx (1-2y)\left\{\left[1 - \frac{\mathrm{R}^2}{360}\, y(1-y)(1+3y-3y^2)\right]\cos nt + \frac{\mathrm{R}}{6}\, y(1-y)\sin nt\right\} + 0(\mathrm{R}^3). \tag{3.4}$$

From (3.3) we have

$$[g(y)]^2 e^{2i\tau} = \frac{\cosh\frac{\lambda}{2} + \cos\frac{\lambda}{2}}{\cosh\lambda - \cos\lambda}\left[\cosh\frac{\lambda}{2}(1-2y) - \cos\frac{\lambda}{2}(1-2y)\right] + \frac{\cosh\frac{\lambda}{2}(1+i) - 1}{\cosh\lambda(1+i) - 1}\left[\cosh\frac{\lambda}{2}(1+i)(1-2y) - 1)\right] e^{2i\tau}, \tag{3.5}$$

and

$$\left[\frac{dg}{dy}\right]^2 e^{2i\tau} = \frac{\lambda^2}{2}\frac{\cosh\frac{\lambda}{2}+\cos\frac{\lambda}{2}}{\cosh\lambda-\cos\lambda}\left[\cosh\frac{\lambda}{2}(1-2y)+\cos\frac{\lambda}{2}(1-2y)\right]$$

$$+\frac{i\lambda^2}{2}\frac{\cosh\frac{\lambda}{2}(1+i)+1}{\cosh\lambda(1+i)-1}$$

$$\times\left[\cosh\frac{\lambda}{2}(1+i)(1-2y)+1\right]e^{2i\tau}. \qquad (3.6)$$

Substitution of (3.5) and (3.6) in equation (2.18) yields the equations necessary for determining the steady and the fluctuating components of the radial-axial flow under the same boundary conditions (2.24) and (2.25). The steady components of the axial and radial flows are

$$f(y) = -\frac{1}{2}\frac{\cosh\frac{\lambda}{2}+\cos\frac{\lambda}{2}}{\cosh\lambda-\cos\lambda}\left\{\left(3S\frac{\lambda^2}{2}-1\right)\left[(3y^2-2y^3)\right.\right.$$

$$\times\left(\frac{2}{\lambda}\sinh\frac{\lambda}{2}-\cosh\frac{\lambda}{2}\right)+\frac{1}{\lambda}\sinh\frac{\lambda}{2}(1-2y)+y\cosh\frac{\lambda}{2}$$

$$\left.-\frac{1}{\lambda}\sinh\frac{\lambda}{2}\right]+\left(3S\frac{\lambda^2}{2}+1\right)\left[(3y^2-2y^3)\left(\cos\frac{\lambda}{2}-\frac{2}{\lambda}\sin\frac{\lambda}{2}\right)\right.$$

$$\left.\left.-\frac{1}{\lambda}\sin\frac{\lambda}{2}(1-2y)-y\cos\frac{\lambda}{2}+\frac{1}{\lambda}\sin\frac{\lambda}{2}\right]\right\}, \qquad (3.7)$$

and

$$f'(y) = \frac{1}{2}\frac{\cosh\frac{\lambda}{2}+\cos\frac{\lambda}{2}}{\cosh\lambda-\cos\lambda}\left\{\left(3S\frac{\lambda^2}{2}-1\right)\left[6(y^2-y)\left(\frac{2}{\lambda}\sinh\frac{\lambda}{2}\right.\right.\right.$$

$$\left.-\cosh\frac{\lambda}{2}\right)-\cosh\frac{\lambda}{2}+\cosh\frac{\lambda}{2}(1-2y)\Big]+\left(3S\frac{\lambda^2}{2}+1\right)$$

$$\times\left[6(y^2-y)\left(\cos\frac{\lambda}{2}-\frac{2}{\lambda}\sin\frac{\lambda}{2}\right)+\cos\frac{\lambda}{2}\right.$$

$$\left.\left.-\cos\frac{\lambda}{2}(1-2y)\right]\right\}. \qquad (3.8)$$

For small Reynolds numbers we have

$$f(y) \approx \frac{R}{60} y^2 (1-y)^2 (1-2y) \left\{ -1 + \frac{R^2}{3 \times 7!} [-3 + 20y \right.$$

$$\left. (y^3 - 2y^2 + 2y - 1)] - \frac{R^2 S}{28} [4y^2 - 4y + 3] \right\} + 0(R^5), \tag{3.9}$$

and

$$f'(y) \approx \frac{R}{30} y(1-y) \left\{ (1 - 5y + 5y^2) + \frac{R^2}{7!} [60 (y^6 - 3y^5 + 4y^4 - 3y^3) \right.$$

$$+ 5y(13y - 1) - 1] - \frac{R^2 S}{28} [7(4y^4 - 8y^3$$

$$\left. + 7y^2 - 3y) + 3] \right\} + 0(R^5). \tag{3.10}$$

The fluctuating component of the radial-axial flow is given by

$$\frac{\lambda(1+i)}{\sqrt{2}} h(y)$$

$$= \frac{iL_1}{2} \left[\frac{\lambda(1+i)}{\sqrt{2}} y - \sinh \frac{\lambda(1+i)}{\sqrt{2}} y \right] + D \frac{\lambda(1+i)}{\sqrt{2}}$$

$$\times \left[1 - \cosh \frac{\lambda(1+i)}{\sqrt{2}} y \right] + \frac{3S \frac{\lambda^2}{4} + \frac{i}{2}}{\cosh \lambda(1+i) - 1}$$

$$\times \left\{ - \frac{\lambda(1+i)}{\sqrt{2}} y + \frac{1}{\sqrt{2}} \sinh \lambda(1+i) \cosh \frac{\lambda}{2}(1+i) \right.$$

$$\times \cosh \frac{\lambda(1+i)}{\sqrt{2}} y - \sinh^2 \frac{\lambda(1+i)}{\sqrt{2}} \sinh \frac{\lambda(1+i)}{\sqrt{2}} y$$

$$\left. - \frac{1}{\sqrt{2}} \cosh \frac{\lambda}{\sqrt{2}}(1+i) \sinh \frac{\lambda}{2}(1+i)(1-2y) \right\}$$

$$+ \frac{\left(3S \frac{\lambda^2}{4} - \frac{i}{2}\right)}{\cosh \lambda(1+i) - 1} \left\{ \frac{1}{\sqrt{2}} \sinh \frac{\lambda}{2}(1+i) \cosh \frac{\lambda(1+i)}{\sqrt{2}} y \right.$$

$$\left. - \frac{\lambda(1+i)}{\sqrt{2}} y \cosh \frac{\lambda(1+i)}{2} - \frac{1}{\sqrt{2}} \sinh \frac{\lambda}{2}(1+i)(1-2y) \right\}, \tag{3.11}$$

where

$$\frac{iL_1}{2}[\cosh\lambda(1+i)-1]\left[2\cosh\frac{\lambda(1+i)}{\sqrt{2}}-2-\frac{\lambda(1+i)}{\sqrt{2}}\sinh\frac{\lambda(1+i)}{\sqrt{2}}\right]$$

$$=\left(3S\frac{\lambda^2}{4}-\frac{i}{2}\right)\left\{\sqrt{2}\sinh\frac{\lambda}{2}(1+i)\sinh\frac{\lambda}{\sqrt{2}}(1+i)-\frac{\lambda(1+i)}{\sqrt{2}}\cosh\frac{\lambda}{2}(1+i)\sinh\frac{\lambda}{\sqrt{2}}(1+i)\right\}$$

$$+\left(3S\frac{\lambda^2}{4}+\frac{i}{2}\right)\left\{\sqrt{2}\sinh\frac{\lambda}{2}(1+i)\cosh\frac{\lambda(1+i)}{\sqrt{2}}\times\sinh\frac{\lambda}{\sqrt{2}}(1+i)+2\sinh^2\frac{\lambda(1+i)}{2}\left(1-\cosh\frac{\lambda(1+i)}{\sqrt{2}}\right)-\frac{\lambda(1+i)}{\sqrt{2}}\sinh\frac{\lambda}{\sqrt{2}}(1+i)\right\}, \tag{3.12}$$

and

$$D[\cosh\lambda(1+i)-1]\left[2\cosh\frac{\lambda(1+i)}{\sqrt{2}}-2-\frac{\lambda(1-i)}{\sqrt{2}}\sinh\frac{\lambda(1+i)}{\sqrt{2}}\right]$$

$$=-\left(3S\frac{\lambda^2}{4}-\frac{i}{2}\right)\left\{\cosh\frac{\lambda}{2}(1+i)\left(1-\cosh\frac{\lambda(1+i)}{\sqrt{2}}\right)+\frac{1}{\sqrt{2}}\sinh\frac{\lambda}{2}(1+i)\sinh\frac{\lambda}{\sqrt{2}}(1+i)\right\}-\left(3S\frac{\lambda^2}{4}+\frac{i}{2}\right)\times\left\{\cosh^2\frac{\lambda}{2}(1+i)\left(1-\cosh\frac{\lambda(1+i)}{\sqrt{2}}\right)+\frac{1}{\sqrt{2}}\sinh\frac{\lambda}{2}(1+i)\cosh\frac{\lambda}{2}(1+i)\sinh\frac{\lambda}{\sqrt{2}}(1+i)\right\}. \tag{3.13}$$

In the present investigation we find that our approximations are valid for small Reynolds numbers only. Figure 3 shows the effect of non-Newtonian term on the typical streamline of the steady flow when both the discs are oscillating in the opposite directions. The flow is symmetrical about

the plane $y = \frac{1}{2}$. Curves are drawn for R = 10 and S = − 0·5, − 0·1, 0, + 0·05. The effect of negative non-Newtonian coefficient is to flatten the streamline and that of the positive non-Newtonian coefficient is to make it more curved. Figure 4 represents the steady component of the radial flow

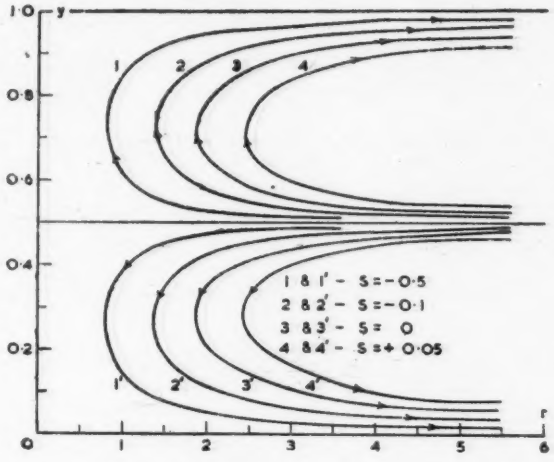

FIG. 3. Two discs oscillating: Streamlines of steady radial-axial flow for R = 10 and S = − 0·5, − 0·1, 0, + 0·05.

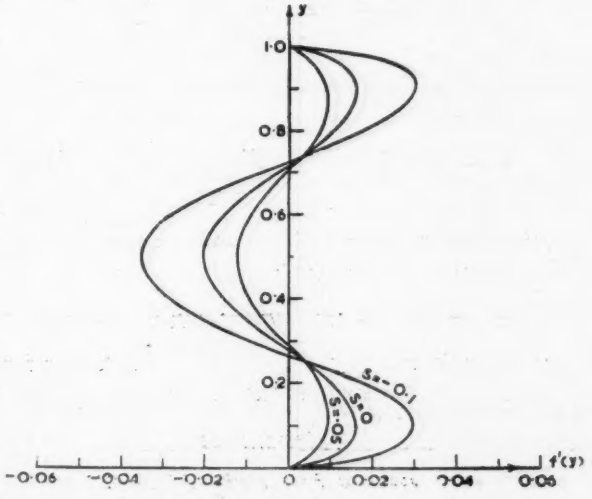

FIG. 4. Two discs oscillating: Steady radial velocity f' for S = − 0·1, 0, + 0·05.

for $S = -0{\cdot}1$, 0 and $+0{\cdot}05$. For $S = -0{\cdot}1$ it is zero on the planes $y = 0{\cdot}26$ and $y = 0{\cdot}72$. There is a radial outflow between these and the walls due to the predominance of centrifugal action. For $0{\cdot}26 < y < 0{\cdot}72$ there is an inflow as the pressure gradient is then the main factor. For $S = +0{\cdot}05$ it is zero on the plane $y = 0{\cdot}29$ and $y = 0{\cdot}71$.

The shearing stresses acting on the discs $z = 0$ and $z = d$ are equal in magnitude but opposite in sign.

For small Reynolds numbers we have the shearing stresses,

$$T_{rz} = \mu \frac{r}{d} \frac{\Omega^2}{n} \frac{R}{120} [4 + R(12S - 1) \sin 2nt] + 0(R^3),$$

$$T_{\theta z} = -2\mu \frac{r}{d} \Omega \left[\left(1 + \frac{R^2}{720}\right) \cos nt - \frac{R}{12} \sin nt\right] + 0(R^3),$$

and

$$T_{r\theta} = -\mu_c \frac{r^2}{d^2} \frac{\Omega^3}{n} \frac{R}{120} \left[8 \cos nt + R\left(12S - \frac{5}{3}\right) \sin nt \right.$$

$$\left. + R(12S - 1) \sin 3nt\right] + 0(R^3).$$

Summary

The flow of an incompressible non-Newtonian viscous fluid contained between two torsionally oscillating infinite parallel discs is investigated. The two specific cases studied are (*i*) one disc only oscillates while the other is at rest and (*ii*) both discs oscillate with the same frequency and amplitude but in opposite directions. Assuming that the amplitude of oscillation, Ω/n, is small and neglecting the squares and higher powers of Ω/n, the equations of motion have been solved exactly for velocity and pressure satisfying all the boundary conditions. The effect of both positive and negative coefficients of cross-viscosity on the steady components of the flow has been represented graphically.

Acknowledgement

The author is highly indebted to Prof. P. L. Bhatnagar for his constant guidance and kind help throughout the preparation of this paper.

Reference

Rosenblat, S. .. *Journ. of Fluid Mech.*, 1960, **8**, 388.

711–61. Printed at the Bangalore Press, Bangalore City, by T. K. Balakrishnan, Superintendent, and Published by The Indian Academy of Sciences, Bangalore.

NOTICE TO AUTHORS

Scientific papers intended for publication in the *Proceedings of the Indian Academy of Sciences* can be accepted only when they are communicated by a Fellow of the Academy whose duty shall be to satisfy himself that such communications are fit to be read at the Meeting of the Academy and published in its *Proceedings*.

Papers should not ordinarily exceed fifty pages of foolscap. MSS. should be either typewritten or written in legible hand on one side of the paper. All papers should be carefully revised by the authors and should be absolutely in final form for printing. Position for text-figures should be indicated. Each paper shall conclude with a critical summary not exceeding 350 words.

Drawings, diagrams or other illustrations should be made on larger scale (preferably) twice the size than the ones in which they are intended to appear. They should be done in Indian ink on bristol board with lettering in pencil. Scale of magnification of camera lucida tracings should be indicated by the side of drawings. In certain special cases arrangements will also be made for monochrome lithographic and other colour plates. Reduction of illustrations desired should be indicated in pencil. Appropriate legends should accompany all drawings. Names of authors are to be marked in pencil on the left-hand corner of drawing sheets. Photomicrographs should be securely mounted with colourless paste.

All tables, quotations and footnotes which will be set hereafter (beginning from Vol. I, No. 2) in types smaller than the text, should be typewritten on separate sheets and placed with the text in proper sequence. Footnotes should be numbered in Arabic numerals.

References to literature in the text should be given, whenever possible, in chronological order, only the names of authors and years of publication, in brackets, being given. They should be cited in full after the summary, the authors' names following in alphabetical order. Thus,

Name or Names of author; Name of Journal (abbreviation) with a single underline; Year of publication; Number of Volume with a double underline, and lastly page. The following would be a useful illustration:—

Bergmann and Stather . . . . . Z. Physiol. Chem., 1926, 152, 189.

Two copies of slip-proof and wherever possible, a page proof for final revision will be sent to authors. All corrections are best made on the slip-proof which should be transmitted to the Office of the Academy. All proof corrections involve heavy expenses which would be negligible if the papers are carefully revised by the authors before submission.

Fifty free reprints including plates and with cover will be supplied for each paper. Additional copies can be supplied at cost on previous intimation.

Blocks appearing in the *Proceedings* will be available for purchase by their respective authors. Orders for the same should be sent along with the corrected proofs and in any case not later than one month after the date of publication of the paper. The price charged would be 25% of the actual cost of the blocks *plus* freight and despatching charges. If the blocks are reproduced in other journals or publications, due acknowledgment should be made in them to the *Proceedings*.

The original drawings and plates of blocks appearing in the *Proceedings* will be returned to such of the authors as may require them provided the cost of despatching such originals is borne by them.

CONTENTS

PAGE

Some Effects of Geomagnetic Activity on the F2 Region of the Ionosphere over Leopoldville (4·4° S, 15·3° E) . . . . . R. G. Rastogi 155

Heterocyclic Compounds. Part XVII. Synthesis of Dihydrofuro (2′ : 3′—2 : 3) Quinoline . . . . . Joseph P. John and P. Shanmugam 161

Heterocyclic Compounds. Part XVIII. Synthetic Experiments in the Quinazoline Series . . . . . M. Krishnan 165

An Approximate Method for the Calculation of the Incompressible Laminar Spanwise Boundary Layer on an Infinite Uniform Yawed Cylinder with Distributed Suction . . . . . Kapildeo Prasad Sinha 171

Flow of Non-Newtonian Fluid between Torsionally Oscillating Discs . . . . . (Miss) G. K. Rajeswari 188